

Mobile Laboratory Measurement of Black Carbon, Particulate Polycyclic  
Aromatic Hydrocarbons and Other Exhaust Emissions in Mexico City

**Mei Jiang**

Thesis submitted to the Faculty of Virginia Polytechnic Institute and State University

in partial fulfillment for the degree of

Master of Science

In

Environmental Science and Engineering

Linsey C. Marr

John C. Little

Douglas J. Nelson

February 2<sup>nd</sup>, 2005

Blacksburg, VA

Key Words: Mobile laboratory, Black carbon, Polycyclic aromatic hydrocarbons,  
Emission inventory, Mexico City

# Mobile Laboratory Measurements of Black Carbon, Particulate Polycyclic Aromatic Hydrocarbons and Other Exhaust Emissions in Mexico City

Mei Jiang

Linsey C. Marr, chair

Department of Civil and Environmental Engineering

## **Abstract**

Black carbon (BC) and polycyclic aromatic hydrocarbons (PAHs) are two atmospheric pollutants produced by motor vehicles using carbonaceous fuels. As a part of the Mexico City Project, measurements of BC, PPAHs and many other gas- and particle-phase emissions were measured in Mexico City using a mobile laboratory during the Mexico City Metropolitan Area field campaign in April 2003 (MCMA-2003). The main goal of this research is to estimate emissions of BC and particulate PAHs (PPAHs) for Mexico City's vehicle fleet. The emissions of gas-phase pollutants such as carbon monoxide (CO), total nitrogen oxides (NO<sub>y</sub>) and volatile organic compounds (VOC) are also estimated. The mobile lab has previously been used to chase vehicles and measure their emissions, but analysis has traditionally focused on determining emission factors of individual vehicles associated with specific chasing events. The laboratory continuously samples ambient air from an inlet at the front of the van, and it is always "seeing" exhaust plumes from the vehicles around it while driving through traffic. We have developed an algorithm that automatically identifies the exhaust plume measurement points, which are then used as the basis for calculation of emission factors. In the nearly 90 hours of on-road sampling during the field campaign, we have identified ~30,000 exhaust measurement points. The large sample size enables us to estimate fleet-average emission factors and thus the emission inventory. Motor vehicles are estimated to emit approximately 1,960 tons year<sup>-1</sup> BC, 56.2 tons year<sup>-1</sup> PPAHs, 1,320,000 tons year<sup>-1</sup> CO, 125,000 tons year<sup>-1</sup> NO<sub>y</sub> and 2440 tons year<sup>-1</sup> VOCs. The spatial and temporal patterns of BC and PPAHs in different locations within MCMA are also studied.

## **Acknowledgements**

I would like to give my most sincere thanks to my advisor, Dr. Linsey Marr, for her consistent encouragement and tireless guidance and direction, and for giving me this great opportunity that led to a very rewarding and fascinating experience. I would also like to express my great appreciation for Drs. John Little and Douglas Nelson for joining my graduate committee, providing guidance and input, and taking time to review my work. This work could not have been accomplished without the guidance and contribution from Edward Dunlea, Scott Herndon, John Jayne, Todd Rogers, Berk Knighton, Miguel Zavala, Luisa Molina and Mario Molina. Thanks to the Alliance for Global Sustainability and the Mexican Metropolitan Environmental Commission to the Integrated Program on Urban, Regional and Global Air Pollution at MIT, who provided funds for this research. I'd also like to thank my colleague, Claire Booth, for her valuable input to my work and the countless help I received from her. Special thanks to my husband, Hao Tan, who has always understood, encouraged, helped and supported me all the way through the process of producing this work.

## Table of Contents

<b>Abstract</b> .....	ii
<b>Acknowledgements</b> .....	iii
<b>List of Figures</b> .....	v
<b>List of Tables</b> .....	vii
<b>General Introduction</b>	
Research Objectives.....	1
Background.....	1
Black Carbon.....	1
PAHs.....	5
Emission Factors.....	7
Previous Studies.....	8
Mexico City Project .....	10
Air Pollution in Mexico City.....	10
Mexico City Project and the MCMA 2003 field campaign.....	10
Mobile Laboratory.....	11
Selected Instruments.....	12
References.....	14
<b>Manuscript: Mobile Laboratory Measurement of Black Carbon, Polycyclic Aromatic Hydrocarbons and Other Exhaust Emissions in Mexico City</b>	
Abstract.....	16
Introduction.....	17
Experimental section.....	19
Results.....	26
Discussion.....	28
Conclusions.....	32
References.....	33
<b>Appendix A.</b> Emission inventory calculations.....	35
<b>Appendix B.</b> Spatial and temporal distributions of BC and PPAHs.....	41
<b>Appendix C.</b> Black carbon QA procedures.....	49
<b>Appendix D.</b> Igor Pro procedures.....	52

## List of Figures

Figure 0.1	Schematic representation of diesel exhaust particles and vapor-phase compounds.....	3
Figure 0.2	Estimated global and U.S. distribution of black carbon emissions.....	5
Figure 0.3	Principle of the Photoelectric Aerosol Sensor.....	13
Figure 1.1	Schematic of the ARI mobile laboratory as instrumented for the MCMA-2003 field campaign.....	20
Figure 1.2	Determination of the natural background variance of CO <sub>2</sub> concentrations based on measurements while the mobile lab was parked.....	22
Figure 1.3	Self-sampling identification.....	23
Figure 1.4	Location of the sampling inlet, van's onboard generator and its own tailpipe.....	24
Figure 1.5	Construction of the exhaust measurement marker time series.....	24
Figure 1.6	Histogram of BC emission factors.....	27
Figure 1.7	Histogram of PPAH emission factors.....	27
Figure 1.8	Histogram of benzene emission factors.....	27
Figure 1.9	Histogram of CO emission factors.....	27
Figure 1.10	Histogram of NO <sub>y</sub> emission factors.....	28
Figure 1.11	Comparison of annual emissions of CO, NO <sub>y</sub> and VOCs using the new mobile lab-based method for the year 2003 versus government estimates for the year 2000.....	30
Figure B.1	Map of the locations of the fixed-site experiments.....	42
Figure B.2a	Black carbon (BC) and PPAH concentrations measured at La Merced during the MCMA-2003 field campaign (PPAH axis shown full-scale)...	44
Figure B.2b	Black carbon (BC) and PPAH concentrations measured at La Merced during the MCMA-2003 field campaign (with the PPAH axis truncated to illustrate more clearly the concentration variations).....	44
Figure B.3a	Black carbon (BC) and PPAH concentrations measured at CENICA during the MCMA-2003 field campaign (April 17 – 18).....	45
Figure B.3b	Black carbon (BC) and PPAH concentrations measured at CENICA during the MCMA-2003 field campaign (April 19 – 20).....	46

Figure B.4	Black carbon (BC) and PPAH concentrations measured at Pedregal during the MCMA-2003 field campaign (April 22-23). . . . .	47
Figure B.5	Black carbon (BC) and PPAH concentrations measured at Santa Ana during the MCMA-2003 field campaign (April 15-16). . . . .	48

## List of Tables

Table 0.1	The main instrumentations in the 2003 ARI mobile lab.....	12
Table 1.1	Emission factors of the measured pollutants from on-road motor vehicles in Mexico City (MCMA-2003).....	26
Table 1.2	Comparison of emission inventories based on the mobile laboratory measurements in spring 2003, government modeling estimates of Mexico City in 2000 and ambient pollutant concentration ratios measured during MCMA-2003.....	30
Table 1.3	Emission factors of BC and PPAHs for gasoline and diesel, or light-duty and heavy-duty vehicles, determined in tunnel experiments and remote sensing studies.....	31
Table A.1	$\Delta P/\Delta CO_2$ ratios of different pollutants for one data point.....	36
Table A.2	Average emission factors in Mexico City's fleet.....	38
Table A.3	2000 Fuel sales in Mexico City and selected fuel properties.....	39
Table A.4	Annual motor vehicle emissions in Mexico City.....	39
Table A.5	Annual BC and PPAH emissions from ambient measurements.....	40
Table B.1	Typical values of 24-hr averages, daily maximum concentrations, nighttime (6 p.m. – 6 a.m.) averages and the period of time when the maximum concentrations are observed (POM) for black carbon at the four experimental sites.....	42
Table B.2.	Typical values of 24-hr averages, daily maximum concentrations, nighttime (6 p.m. – 6 a.m.) averages and the period of time when the maximum concentrations are observed (POM) for PPAHS at the four experimental sites.....	43
Table C.1	Data flags used for the QA-ed black carbon data .....	51

## **General Introduction**

### **1. Research objectives**

Black carbon (BC) and particulate polycyclic aromatic hydrocarbons (PPAHs) are two combustion byproducts that are often formed together and of critical concern because of their effects on human health, urban air quality and climate change. As part of an integrated case study of megacity air quality, the Mexico City Project, a five-week field measurement campaign was launched in April 2003. This research focuses on the measurements of BC and PPAHs collected by a mobile laboratory during the field campaign and aims to quantify their emissions from vehicle sources in Mexico City. As notorious as the air quality is in Mexico City, emissions of these two important pollutants have never before been estimated for the megacity. The specific objectives of this research are:

- (1) to characterize the emission factors of black carbon and PPAHs from the vehicle fleet in Mexico City Metropolitan Area (MCMA);
- (2) to estimate the annual total emissions of black carbon and PPAHs from mobile sources;
- (3) to analyze the spatial distribution and diurnal patterns of black carbon and PPAHs in the MCMA.

A key component of this research is the development of a new method to characterize fleet-average emissions. Detailed methods and results pertaining to motor vehicle emission estimates and to the spatial and temporal patterns of black carbon and PPAH concentrations in Mexico City are presented in subsequent chapters.

### **2. Background**

This section provides introductory information on the definition, atmospheric effects, sources and fates of black carbon and PAHs. The Mexico City Project and the MCMA-2003 field campaign are also described.

#### **2.1 Black carbon**

##### **2.1.1 Definition**

For a precise understanding of black carbon, it is helpful to know the relationship between black carbon and soot. Soot is the black particulate matter that is formed as an undesirable byproduct of combustion of organic materials, such as coal, wood, fuel oil, waste oil, paper, plastics and household refuse. The chemical composition and properties of soot particles are highly variable and depend on the type of starting material and the combustion conditions. In general, soot has a total carbon content of <60%, with inorganic material and/or soluble organics making up a large fraction of the particles. The carbon can be separated into two major categories: black carbon (BC), also referred to as elemental carbon (EC), and organic carbon, such as PAHs (HHS 2002). In many cases, black carbon is also directly referred to as soot. The definition of black carbon is largely based on operational and analytical considerations: “it is the portion of combustion emissions that is insoluble in both polar and non-polar solvents, and stable in air or oxygen at temperatures up to approximately 350 - 400°C, and it is strongly optically absorbing.” (Hansen 2003)

### **2.1.2 Effects**

Black carbon in the atmosphere has numerous effects, described in the following sections.

#### **a. Physiological effects**

Due to its high porosity, black carbon has the ability to adsorb other species from the vapor phase, especially organics. Figure 0.1 shows the structure and composition of typical diesel exhaust aerosol. Carbonaceous particulate matter is the most notorious pollutant from diesel engines because it is highly visible in the exhaust, but the potentially carcinogenic organic compounds adsorbed on the particle surfaces are in fact a greater concern from the standpoint of public health. Particulate black carbon, in the form of solid carbon spheres ranging in size from 0.01 to 0.08  $\mu\text{m}$  in diameter, serves as the nuclei of agglomerated particles which are coated by adsorbed hydrocarbons. Small particles composed of liquid condensed hydrocarbons or hydrated sulfates are also associated with the aggregates (Sawyer et al.1995).

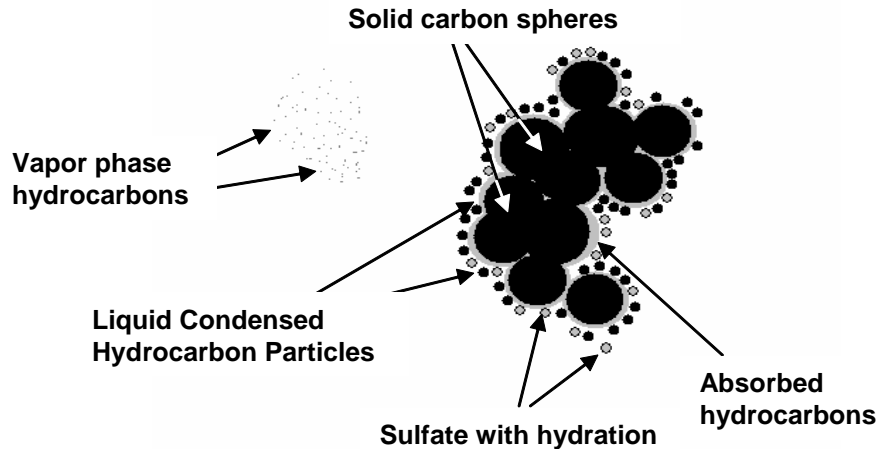


**Figure 0.1** Schematic representation of diesel exhaust particles and vapor-phase compounds (Adapted from Sawyer *et al.* 1995).

Black carbon particles, regardless of their source, are always associated with a variety of known or potential carcinogens such as arsenic, cadmium, chromium, nickel, benzo[a]anthracene, benzo[a]pyrene, dibenzo[a,h]anthracene, and indeno[1,2,3-cd]pyrene. Since the vast majority of black carbon resides in the fine fraction of particulate matter (e.g. PM<sub>2.5</sub>, particles with aerodynamic diameter < 2.5 μm), it can be readily inhaled and deposited deep in human lungs. Such particles may therefore act as vehicles for the transport and localized deposition of harmful compounds to the human pulmonary system. There is much epidemiological evidence that supports a link between PM<sub>2.5</sub> and adverse health effects. The physiological effects related to black carbon will be described in section 2.2.2 that focuses on PAHs, because it is actually the PAHs adsorbed on black carbon particles that are believed to be the direct threat to human health.

### **b. Physical effects**

Black carbon has a large optical absorption cross-section, which leads to the extinction of radiation, both infrared and visible. When black carbon deposits to snow and ice surfaces, their surface albedos may be reduced sufficiently to accelerate springtime thawing. In heavily polluted cities like Mexico City, the decrease of visible radiation because of black carbon produces brown skies and reduced visibility. It is also widely accepted that increased emissions of black carbon contribute to global warming by increasing the

optical depth (a measure of optically absorbing materials) of the atmosphere. In fact, the warming effect of black carbon in the atmosphere is gaining more and more recognition. Recent modeling studies suggest that reducing the emissions of black carbon may be one of the most effective solutions in slowing global warming (Hansen *et al.* 2000; Jacobson 2002; Menon *et al.* 2002).

### **c. Microphysical effects**

The ability of fine particles to remain in the atmosphere for long periods of time may allow them to be transported to remote unpolluted regions of the atmosphere. Although fresh black carbon particles are always hydrophobic, their surfaces can be modified chemically during transport so that the supersaturation necessary for condensation is reduced. Under such circumstances, black carbon particles may act as cloud condensation nuclei (CCN), altering the coverage, density and rainfall potential of clouds, and reducing the albedo of clouds. These effects can perturb regional “atmospheric stability and vertical motions” and consequently affect the “large-scale circulation and hydrologic cycle,” and cause significant regional climate changes (Menon *et al.* 2002). It has been claimed that the radiative forcing by brown haze, which is significantly amplified by its black carbon content, in south Asia is large enough to perturb the rainfall patterns over the tropical Indian Ocean and the surrounding areas (Ramanathan *et al.* 2002). Menon *et al.* interpret the increased summer floods in south China, increased drought in north China, and moderate cooling in China and India, while most of the world has been warming, as an effect of the vast emissions of anthropogenic black carbon produced by household burning of biomass and coal, which are particularly common in China and India.

#### **2.1.3 Sources and fates**

The major sources of aerosol black carbon can be grouped into three broad categories: (1) combustion of fossil fuels; (2) biomass burning; and (3) naturally-occurring forest fires. The first two of the above categories represent anthropogenic activities. On a global scale, these sources are believed to be the major input to the atmospheric emission of black carbon. Although forest fire emissions are copious and can be locally overwhelming, they are not considered to be a major contributor to the atmospheric

burden of black carbon on a global, year-round basis (Ramanathan *et al.* 2002; Hansen 2003). Some other processes also contribute to black carbon emissions, such as industries like metals processing, asphalt manufacturing, petroleum refining, oil and gas production, rubber and plastics production, fugitive dust and agricultural sources like tilling and livestock (Battye *et al.* 2002). According to a report sponsored by the U.S. Department of Energy, the global total of black carbon emissions is approximately 12.6 Tg C y<sup>-1</sup> (Dignon *et al.* 1994). Figure 0.2 shows an estimate of global and U.S. distributions of black carbon sources.

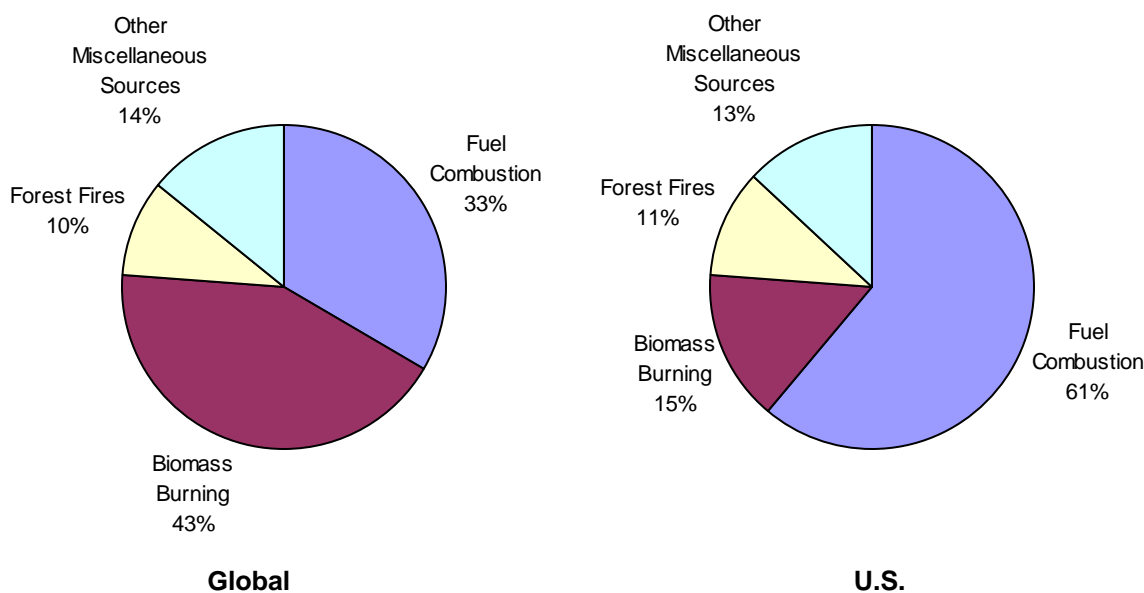


**Figure 0.2** Estimated global and U.S. distribution of black carbon emissions (Battye *et al.* 2002).

Aerosol black carbon is removed from the atmosphere by wet and dry deposition. Removal rates will depend on the particle's size and its likelihood of being involved in condensation and precipitation processes. An annual average lifetime of aerosol black carbon is estimated to be  $6.5 \pm 4.8$  days (Reddy *et al.* 1999).

## 2.2 PAHs

### 2.2.1 Definition

PAHs are a group of over 100 different compounds that are composed of two or more fused aromatic rings, such as naphthalene and benzo(a)pyrene. Like black carbon, PAHs are formed as a byproduct of incomplete combustion of organic materials. Because of

their semivolatile nature, PAHs are found both in the gas-phase and particle-phase in the atmosphere. PAHs and black carbon are always formed together in combustion processes. It is believed by some that PAHs are the molecular precursors of soot particle or a side branch in the soot formation process (Siegmann *et al.* 1998). Most PAHs have no known use, but a few are produced deliberately and used to make medicines, dyes, plastics, and pesticides.

### **2.2.2 Effects**

Although PAHs are exceedingly stable molecules, some of them have been found to be physiologically active. Benzo(a)pyrene (BaP), for example, is known as a potential carcinogenic substance that can contribute to the development of cancer cells in humans. Animal experiments show that short-term exposure to large doses of BaP can damage red blood cells and suppress the immune system, while long-term exposure to smaller doses can have developmental and reproductive effects. Reports in humans indicate that people exposed by inhalation and skin contact to PAHs for extended periods can develop cancer at a higher rate than normal (ATSDR 1995; USEPA 1995). Human exposure to PAHs can occur by breathing contaminated air, eating foods that have been grilled or smoked, or by smoking tobacco products. Because PAHs are produced as byproducts in so many industrial processes, occupational exposure can often occur. Evidence for an increased skin cancer risk, particularly of the scrotum, is demonstrated by numerous case reports, dating back over 200 years, among chimney sweeps. More recent cohort studies of mortality among chimney sweeps have shown a significantly increased risk of lung cancer (HHS 2002). PAHs are also suspected to be endocrine disruptors (TBCF 2004).

### **2.2.3 Sources and fates**

PAHs have large natural as well as anthropogenic sources. An EPA estimate of air releases includes wildfires and prescribed burnings as the third largest source (USEPA 1998), although the estimate did not consider the amount produced by volcanoes. Anthropogenic sources of PAHs include fires and a wide range of industrial products and wastes such as coal tar, creosote, waste oils, and wood-treating residues. Major industrial sources of PAHs include primary metals processors, petroleum refineries, paper manufacturers, chemical manufacturers, and plastics manufacturers (TBCF 2004). There

are higher concentrations of PAHs near urban sources; the background level in air in urban areas can be ~10 times that in rural areas. The most important sources of PAHs in urban areas are residential wood combustion, tobacco smoking and food cooking such as meat grilling, but most of all, motor vehicle emissions, especially from light-duty gasoline vehicles (Lobscheid *et al.* 2004). This recent result contradicts the common perception that heavy-duty diesel-powered vehicles are the main source of PAHs in urban areas.

Because they have so many sources, PAHs are found widely throughout the environment. The presence of PAHs in areas far from sources indicates that they are reasonably stable in the atmosphere and capable of long-distance transport. Most PAHs do not dissolve readily in water, but some evaporate from water into the air and they stick strongly to soil or sediment. Tests of PAH biodegradation have resulted in a wide range of soil half-lives from 2 days to 1.9 years (Bradley *et al.* 1994). Furthermore, BaP bioaccumulates in some aquatic organisms that do not have a metabolic detoxification enzyme system to remove it.

### **2.3 Emission factors**

Emission factors relate the quantity of a pollutant released to the atmosphere with the amount of activity associated with the process releasing that pollutant. For example, the emission factor of sulfur dioxide from coal combustion in a power plant is about 3000 g GJ<sup>-1</sup> deliverable energy. Such factors are used to estimate the emissions from various sources of air pollution. Vehicle emission factors are conventionally expressed in mass of pollutants emitted per mile or kilometer traveled. Fuel-based emission factors, however, are defined in units of mass of pollutants per unit mass or volume of fuel consumed. While distance-based emission factors are not applicable to all driving conditions, fuel-based emission factors are thought to be less dependent on driving conditions. For example, while at idle, a vehicle is producing emissions and consuming fuel but traveling zero distance. In this case, a distance-based emission factor is meaningless.

Emission factors for motor vehicles are traditionally measured through dynamometer testing. Vehicles are driven on rollers with resistance according to a prescribed pattern of acceleration, cruising, deceleration, and idling; meanwhile, samples of their emissions are

collected and analyzed in a laboratory. Due to the nature and cost of this type of testing, only a very small sample of vehicles can be tested. Given the skewed distribution of emission factors in the vehicle fleet, it is difficult to obtain a representative value of the fleet average through dynamometer testing. Furthermore, the driving cycle on a dynamometer is not necessarily representative of real-world driving conditions.

To augment dynamometer tests, researchers have conducted tunnel and remote sensing studies of vehicles as they are driven on-road. While tunnel studies usually capture a single emission factor representing the entire fleet, remote sensing studies measure instantaneous emissions from numerous individual vehicles. Both these methods are limited in the range of driving conditions that can be monitored. Long tunnels are scarce and typically represent highway driving. Remote sensing requires a single lane of traffic with high engine load, typically a highway on-ramp. In contrast, a recently developed method involves a mobile laboratory, mostly in the form of a van, truck, boat or airplane, which maneuvers through traffic and chases vehicles to measure their fresh emissions. Mobile labs are able to capture emissions from a large number of vehicles under a wide range of real-world driving conditions.

### **3. Previous studies**

This section reviews previous measurements of black carbon and PAH emission factors. Hansen et al. used an aethalometer and a nondispersive infrared analyzer to measure black carbon and CO<sub>2</sub> concentrations in the plumes of vehicles passing by a fixed location, and the black carbon emission factors were calculated for individual vehicles (Hansen *et al.* 1990). The results show that some vehicles emit a thousand times more black carbon than others, with the emission factors spanning a range of greater than two orders of magnitude, from  $4 \times 10^{-6}$  to  $10^{-3}$  grams of black carbon per gram of carbon in the fuel. The researchers also derived how fuel-based emission factors can be calculated using the ratio of black carbon to CO<sub>2</sub> measured in the diluted vehicle plumes.

Weingartner et al. measured PM<sub>3</sub> and the black carbon and particulate PAH (PPAH) content of the particles in a 3-km-long freeway tunnel (Weingartner *et al.* 1997). They reported the emission factors of PM<sub>3</sub> for gasoline and diesel vehicles separately, and the fraction of black carbon and PPAH content of the diesel PM<sub>3</sub> was found to be 31% and

0.86%. If we assume an average fuel economy of 10 mi gal<sup>-1</sup> for the particular composition of diesel vehicles monitored in this research, including heavy-duty trucks, delivery vans and passenger cars, then these measurements correspond to fuel-based emission factors of 0.48 g BC kg<sup>-1</sup> fuel and 13.4 mg PPAH kg<sup>-1</sup> fuel.

Miguel et al. measured on-road emissions of PPAHs and black carbon from gasoline and diesel vehicles in the Caldecott Tunnel (Miguel *et al.* 1998). Light-duty vehicles and heavy-duty diesel trucks emitted, respectively,  $30 \pm 2$  and  $1440 \pm 160$  mg of BC per kg of fuel burned. Their results showed that diesel trucks were the major source of smaller molecular weight PAHs, whereas light-duty gasoline vehicles were the dominant source of higher molecular weight PAHs, such as benzo[a]pyrene and dibenz[a,h]anthracene.

Kirchstetter et al. conducted a similar study at the Caldecott Tunnel the following year (Kirchstetter *et al.* 1999). Instead of using only time-integrated samples as the previous Caldecott Tunnel study did, they used a condensation nucleus counter, an optical counter and an aethalometer to continuously measure particle properties like number concentrations and mass equivalence. They continued to use integrated samples for the chemical analysis of particles. They concluded that heavy-duty diesel trucks emitted 24 and 37 times more fine particles and black carbon per unit mass of fuel burned than did light-duty vehicles. Heavy-duty diesel trucks also emitted 15-20 times the number of particles per unit mass of fuel burned compared to light-duty vehicles. Fine particle emissions from both vehicle classes were composed mostly of carbon; diesel-derived particulate matter contained more black carbon ( $51 \pm 11\%$  of PM<sub>2.5</sub> mass) than did light-duty fine particle emissions ( $33 \pm 4\%$ ).

A study conducted by Zhu et al. measured the concentrations of black carbon, CO and particle number with increasing distance from the freeway (Zhu et al. 2002). The average concentration of black carbon at 17 m downwind from the freeway was  $23 \mu\text{g m}^{-3}$ . The study also suggested that CO, black carbon and particle number concentrations tracked each other very well. This result supported the conclusion from a previous study that any one of the three pollutants could be used interchangeably to estimate the relative concentration of the other two pollutants near freeways.

## **4. Mexico City Project**

### **4.1 Air pollution in Mexico City**

The Mexico City Metropolitan Area (MCMA) includes Mexico City and a number of municipalities of the neighboring State of Mexico. It sits at an altitude of 2240 m above mean sea level, and spreads over 5000 km<sup>2</sup> of the Mexican plateau. The surrounding mountain ridges make the elevated basin roughly 800 -1000 m deep and effectively trap the atmospheric pollutants produced in this area. The meteorological conditions, featuring strong inversions and intense solar radiation, favor the photochemical formation of ozone. Added to these unmanageable natural factors, nearly 20 million residents, 3.5 million vehicles, and 35,000 industries consume daily more than 40 million liters of fuel (Molina *et al.* 2002), making the transportation sector an extremely important source of air pollution in this area. According to the 1998 emissions inventory, mobile sources contribute nearly all of the CO, about 80 percent of the NO<sub>x</sub>, 40 percent of the hydrocarbons (HC), 20 percent of the SO<sub>2</sub>, and 35 percent of the PM<sub>10</sub> (particulate matter of aerodynamic diameter 10 μm and less) emitted in the MCMA (CAM 2001). Apart from the huge number of vehicles and amount of fuel consumed, the situation is especially exacerbated by congestion, lack of emission control and poor fuel quality.

Having recognized the air pollution problem as a major social concern, the city has undertaken a series of measures to control the emissions since the mid-1980s, such as fuel reformulation, enforcement of a vehicle inspection and maintenance program and the “no-driving day” program. While these efforts successfully reduced the concentrations of some pollutants such as lead, CO and SO<sub>2</sub> to a significant extent, some of the other air quality standards are still frequently violated. For example, the ozone standard has been exceeded on ~80% of the days every year since 1988, and the daily standard for PM<sub>10</sub>, which used to be violated on more than 40% of the days in some years, is still exceeded on ~10% of the days (Molina *et al.* 2002; Molina *et al.* 2004).

### **4.2 Mexico City Project and the MCMA 2003 field campaign**

The Mexico City Project includes a variety of interrelated studies in health impacts, atmospheric science, transportation, economics, technology, and policy, aiming to “provide objective, balanced assessments of the causes and alternative cost-effective

solutions to urban, regional and global air pollution problems” (Molina *et al.* 2002). The project involves a multidisciplinary group of researchers from a wealth of institutions from Mexico, the United States and Europe, and active collaboration with Mexican government officials and decision makers. As the main effort to support the understanding of the air pollution problem in the city, the five-week MCMA-2003 field campaign was launched in Spring 2003 to conduct measurements and modeling studies of atmospheric pollutants in the Mexico City Metropolitan Area. Such an understanding will not only help to build a scientific basis for developing emissions control strategies in the MCMA, but will also provide insights to air pollution problems in other megacities in the world.

The MCMA-2003 field measurement campaign was scheduled to capture the peak season of photochemical activity in this area, but to avoid the rainy season. A major feature of the campaign was the use of a mobile laboratory to measure air quality at different locations around the city and to chase vehicles and measure their emissions. The mobile laboratory was developed at Aerodyne Research, Inc. (ARI) and equipped with a range of real-time particle and trace gas analyzers. Table 0.1 presents the main instruments and the corresponding pollutants that were measured.

Ambient measurements were also conducted at fixed sites, including a highly instrumented “supersite” where a suite of sophisticated monitoring equipment was housed in the National Center for Environmental Research and Training (Centro Nacional de Investigación y Capacitación Ambiental or CENICA). The mobile laboratory also spent time at a few other locations in Mexico City, including La Merced (near downtown), Pedregal (a downwind suburb) and Santa Ana (at the downwind boundary of the Mexico City air basin). When not involved in mobile mapping, chasing or other off-site experiments, the mobile laboratory was sited at CENICA, where its instrument suite contributed to the supersite’s database.

### **4.3 Mobile laboratory**

The mobile laboratory deployed in the MCMA-2003 field campaign is a large van equipped with numerous instruments measuring gaseous and particulate concentrations. The instrumentation and its layout in the 2003 ARI mobile lab are shown in Table 0.1.

**Table 0.1** The main instrumentation in the 2003 ARI mobile lab.

Instrumentation	Measures
Proton Transfer Reaction Mass Spectrometer (PTR-MS)	Speciated volatile organic compounds (VOC)
Tunable Infrared Laser Differential Absorption Spectroscopy (TILDAS)	CH <sub>2</sub> O, CO, NO, NO <sub>2</sub> /HONO – possible pairs: CH <sub>2</sub> O-CO, NO-NO <sub>2</sub> /HONO, CH <sub>2</sub> O-NO <sub>2</sub> /HONO, NO-CO
Aerosol Mass Spectrometer (AMS)	Fine aerosol size distributions and non-refractory chemical composition
Aethalometer (Magee Scientific AE-16)	Black carbon
Aerosol photometer (TSI DustTrak 8520)	PM <sub>2.5</sub>
Photoemission aerosol sensor (EcoChem PAS 2000 CE)	Particulate PAH
Non-dispersive Infrared (NDIR) unit (LICOR)	CO <sub>2</sub>
Condensation Particle Counter (CPC) (TSI 3022)	10 – 1000 nm Particle Number Density
Chemiluminescence and IR and UV absorption	NO/NO <sub>2</sub> , CO and O <sub>3</sub>
Portable canister samplers (at selected sampling points) & gas chromatography with flame ionization (GC-FID) detection	Speciated VOC

#### 4.4 Selected instruments

##### 4.4.1 Aethalometer

Black carbon is measured using an optical absorption instrument, known as aethalometer. The AE-16 Aethalometer (Magee Scientific Company) collects aerosol samples continuously on a quartz fiber filter, and measures the increment of optically absorbing material collected per unit volume of sampled air. The optical attenuation due to the aerosol deposited on the filter is measured by detection of the intensity of light at 880 nm transmitted through the deposition spot on the filter. Since black carbon is the dominant

optically absorbing material at this wavelength, the measurement is interpreted as a mass of black carbon according to calibrations performed by intercomparison with chemical analysis techniques (Hansen 2003). The time resolution of this model can be set from 1 hour to 1 second, depending on the desired sensitivity and actual concentration range.

#### 4.4.2 Photoelectric aerosol sensor

The particle-phase PAH concentration is measured by the EcoChem 2000 CE Photoelectric Aerosol Sensor (PAS) with a time resolution of 10 seconds. The PAS is based on the photoelectric ionization of PAH. When a particle with a layer of condensed or adsorbed PAH on the surface is exposed to UV light that has an energy level higher than the photoelectric threshold of PAHs, the particle emits an electron. The wavelength is selected to ionize the PAH-coated aerosols, while leaving gas molecules and non-carbon aerosols neutral. After photoemission, the original donor particle becomes a positively charged particle, as shown in Figure 0.3. A free gas molecule or another charged particle can capture the photoelectron emitted from the irradiated particle. Because the probability of electron recapture is high for large particles, photoemission is especially effective for particles smaller than 1  $\mu\text{m}$ . The charged particles are then collected on a filter inside an electrometer, where the accumulation of charge is measured. The resultant electric current produces a signal proportional to the concentration of total particle-bound PAH.

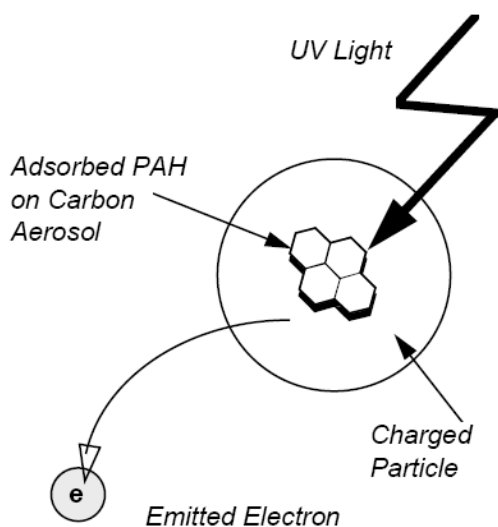


**Figure 0.3** Principle of the Photoelectric Aerosol Sensor. (reprinted with permission from *User's Guide, Realtime PAH monitor, PAS 2000CE*, by EcoChem Analytics)

## References

- ATSDR (1995). Agency for Toxic Substances and Disease Registry. Toxicological Profile for Polycyclic Aromatic Hydrocarbons.
- Battye, W., Boyer, K., Pace, T. G., (2002). "Methods of Improving Global Inventories of Black Carbon and Organic Carbon Particulates." 11th International Emission Inventory Conference.
- Bradley, L. J. N., Magee, B.H., Allen, S.L., (1994). "Background Levels of Polycyclid Aromatic Hydrocarbons (PAH) and Selected Metals in New England Urban Soils." *Journal of Soil Contamination* **3**(4).
- Hansen, A. D. A., Rosen, H., (1990). "Individual Measurements of the Emission Factor of Aerosol Black Carbon in Automobile Plumes." *Air Waste Manage, Assoc.* **40**: 1654-1657.
- Hansen, A. D. A. (2003). The Aethalometer, Magee Scientific Co.
- Hansen, J., Sato, M., Ruedy R., Lacis, A., Oinas, V., (2000). "Global warming in the twenty-first century: An alternative scenario." *PNAS (Proceedings of the National Academy of Sciences of the United States of America)* **97**(18): 9875-9880.
- HHS, U. S. Department of Health and Human Services, Public Health Services, National Toxicology Program, (2002). Report on Carcinogens, Tenth Edition.
- Jacobson, M. Z. (2002). "Control of fossil-fuel particulate black carbon and organic matter, possibly the most effective method of slowing global warming." *Journal of Geophysical Research - Atmospheres* **107**(D19): Art. No. 4410.
- Kirchstetter, T. W., Harley, R. A., Kreisberg, N. M., Stolzenburg, M. R., Hering, S. V., (1999). "On-road measurement of fine particle and nitrogen oxide emissions from light- and heavy-duty motor vehicles." *Atmospheric Environment* **33**: 2988-2968.
- Lobscheid, A. B., McKone, T.E., (2004). "Constraining uncertainties about the sources and magnitude of polycyclic aromatic hydrocarbon (PAH) levels in ambient air: the state of Minnesota as a case study." *Atmospheric Environment* **38**(33): 5501-5515.
- Menon, S., Hansen, J., Nazarenko, L., Luo, Y.F., (2002). "Climate effects of black carbon aerosols in China and India." *Science* **297**(5590): 2250-2253.
- Miguel, A. H., Kirchstetter, T. W., Harley, R. A., Hering, S. V., (1998). "On-road Emissions of Particulate Polycyclic Aromatic Hydrocarbons and Black carbon from Gasoline and Diesel Vehicles." *Environmental Science and Technology* **32**: 450-455.
- Molina, L. T., Molina, M.J., (2002). *Air Quality in the Mexico Megacit: An Integrated Assessment*. Boston, Kluwer Academic Publishers.

Molina, L. T., Molina, M.J., (2004). "Improving Air Quality in Megacities: Mexico City Case Study." *Annals of the New York Academy of Sciences* **1023**(142-158).

Ramanathan, V., Crutzen, P.J., Mitra A. P., Sikka, D., (2002). "The Indian Ocean Experiment and the Asian Brown Cloud." *Current Science* **83**(8): 947-955.

Reddy, M. S., Venkataraman, C., (1999). "Direct radiative forcing from anthropogenic carbonaceous aerosols over India." *Current Science* **76**(7): 1005-1011.

Sawyer, R. F., Johnson, J. H., (1995). "Diesel Exhaust: A Critical Analysis of Emissions, Exposure, and Health Effects." 70.

Siegmann, K., Siegmann, H.C., (1998). "Current Problems in Condensed Matter." Moran-Lopez, (Ed.).

TBCF, The Breast Cancer Fund, (2004). *Chemical Fact Sheets: Polycyclic Aromatic Hydrocarbons*.

USEPA (1995). *Technical Factsheet on: Polycyclic Aromatic Hydrocarbons*. National Primary Drinking Water Regulations.

USEPA (1998). *1990 Emissions Inventory of Section 112(c)(6) Pollutants: Polycyclic Organic Matter (POM), TCDD, TCDF, PCBs, Hexachlorobenzene, Mercury, and Alkylated Lead: Final Report.*, Office of Air and Radiation.

Weingartner, E., Keller, C., Stahel, W. A., Burtscher, H., (1997). "Aerosol Emission in a Road Tunnel." *Atmospheric Environment* **31**(3): 451-462.

Zhu, Y. F., Hinds, W.C., Kim, S., Shen, S., Sioutas, C., (2002). "Study of ultrafine particles near a major highway with heavy-duty diesel traffic." *Atmospheric Environment* **36**: 4323-4335.

## **Manuscript: Mobile Laboratory Measurement of Black Carbon, Polycyclic Aromatic Hydrocarbons and Other Exhaust Emissions in Mexico City**

### **Abstract**

Black carbon (BC) and polycyclic aromatic hydrocarbons (PAHs) are two atmospheric pollutants produced by motor vehicles using carbonaceous fuels. The main goal of this research is to estimate emissions of BC and particle-phase PAHs (PPAHs) for Mexico City's vehicle fleet. The emissions of gas-phase pollutants such as carbon monoxide (CO), total nitrogen oxides (NO<sub>y</sub>) and volatile organic compounds (VOCs) are also estimated. As a part of the Mexico City Metropolitan Area field campaign in April 2003 (MCMA-2003), a mobile laboratory was driven throughout Mexico City. The laboratory is equipped with a comprehensive suite of gas and particle analyzers, including an aethalometer that measures BC and a photoemission aerosol sensor that measures PPAHs. The mobile lab has previously been used to chase vehicles and measure their emissions, but analysis has traditionally focused on determining emission factors of individual vehicles associated with specific chasing events. In this measurement, the laboratory continuously samples ambient air from an inlet at the front of the van, and it is always detecting exhaust plumes from the vehicles around it while driving through traffic. We have developed an algorithm that automatically identifies the exhaust plume measurement points, which are then used as the basis for calculation of emission factors. In the approximately 75 hours of on-road sampling during the field campaign, we have identified over 30,000 exhaust measurement points. The large sample size enables us to estimate fleet-average emission factors and thus the emission inventory. Motor vehicles are estimated to emit approximately 1,960 tons year<sup>-1</sup> BC, 56.2 tons year<sup>-1</sup> PPAHs, 1,320,000 tons year<sup>-1</sup> CO, 125,000 tons year<sup>-1</sup> NO<sub>y</sub> and 2440 tons year<sup>-1</sup> VOCs. The distributions of emission factors for BC and PPAHs are highly skewed, while those for benzene and NO<sub>y</sub> are less skewed.

**Key words:** Mobile laboratory, emission inventory, black carbon, polycyclic aromatic hydrocarbon, total nitrogen oxides (NO<sub>y</sub>), carbon monoxide, benzene, volatile organic compound (VOC).

## Introduction

Mexico City has become known for its air pollution problem as a result of the rapid growth of population, industry, and services, which encouraged an enormous increase in transportation activity. In the 1990s, the Mexican government implemented pollution control measures on vehicles and fuels, which successfully reduced the ambient concentrations of some pollutants such as lead (Pb), carbon monoxide (CO), and sulfur dioxide (SO<sub>2</sub>). Nonetheless, some of the air quality standards are still frequently violated. For example, the ozone standard has been exceeded on ~80% of the days every year since 1988, and the daily standard for PM<sub>10</sub> (particulate matter of aerodynamic diameter 10 μm and less), which used to be violated on more than 40% of the days in some years, is still exceeded on ~10% of the days as to the year 1999, although other monitored pollutant concentrations usually fall below the air quality standard (Molina *et al.* 2002; Molina *et al.* 2004).

As in most large cities, the transportation sector in Mexico City is a major source of air pollution. In addition to the huge number of vehicles and amount of fuel they consume, the situation is especially exacerbated by factors like congestion, lack of emission controls on many vehicles and poor fuel quality. According to the government's 1998 emissions inventory, mobile sources contribute nearly all CO, ~80% of the nitrogen oxides (NO<sub>x</sub>), 40% of the hydrocarbons (HC), 20% of the SO<sub>2</sub> and 35% of the PM<sub>10</sub> emitted in the Mexico City Metropolitan Area (MCMA) (CAM 2001). A field campaign was launched in Spring 2003 to support the understanding of the air pollution problem in Mexico City by conducting measurements and modeling studies of the atmospheric pollutants. In this work, we focus on black carbon (BC) and particulate polycyclic aromatic hydrocarbons (PPAHs), for which the emission inventory has not yet been systematically estimated.

Black carbon refers to the elemental carbonaceous substance in the particulate matter that is formed through incomplete combustion of organic substances. Besides its direct effect on visibility, aerosol black carbon also influences global and regional climate and public health. Recent modeling studies have postulated that BC is a very important component

causing short-term regional cooling but long-term global warming effects on climate (Jacobson 2002). Furthermore, due to the porosity of BC particles and their correspondingly large surface area, BC can adsorb a variety of chemicals that are present in combustion exhaust, including some polycyclic aromatic hydrocarbons (PAHs), which are believed to be carcinogenic or mutagenic (Finlayson-Pitts *et al.* 2000). BC, therefore, is believed to be a human health threat because of its ability to transport carcinogens to the lungs.

PAHs are a group of over 100 different compounds that are composed of two or more fused aromatic rings. They are also a byproduct of incomplete combustion, and are found in both gas and particle phases. Some PAHs, such as benzo(a)pyrene (BaP), have been found to be carcinogenic (Denissenko *et al.* 1996). Animal experiments show that short-term exposure to large doses of BaP can cause red blood cell damage and suppress the immune system, while long-term exposure to smaller doses can have developmental and reproductive effects. Reports in humans indicate that people exposed by inhalation and skin contact to PAHs for a long time can develop cancer at a higher rate than normal (ATSDR 1995; USEPA 1995). Major urban sources of PAHs include residential wood combustion, tobacco smoking and food cooking such as meat grilling, and most of all, motor vehicle emissions. Contrary to the perception that diesel vehicles are the main vehicular source of PAHs, light-duty gasoline vehicles are found to be the most important source for PAHs emission in certain urban areas because of their overwhelmingly large amount of activity (Lobscheid *et al.* 2004). While motor vehicles are commonly believed to be the predominant source for both PAHs and BC in urban areas like MCMA, more accurate measurements are necessary for the quantification and understanding of this important source.

A variety of methods are used to measure motor vehicle emissions, including chassis dynamometer, tunnel measurement, remote sensing and mobile laboratory studies. A chassis dynamometer is ideal for quantifying emissions from individual vehicles under a range of controlled driving conditions. However, dynamometer testing is possible for only a limited sample size, and thus it is difficult to represent the entire fleet and to estimate the emission inventory accurately. Tunnel and remote sensing studies can

provide average fleet emission values by sampling a larger number of vehicles, but because the measurements are conducted at a fixed site, they are usually restricted to certain driving conditions. Mobile laboratories, which are instrumented mobile platforms, including vans, trailers, boats and airplanes (Kolb *et al.* 2004), can measure fresh tailpipe emissions while tailing vehicles, through which emission estimates can be made for both individual vehicles and the entire fleet under a wide variety of real-world driving conditions.

During the MCMA-2003 field campaign a mobile laboratory was deployed to chase vehicles, park at fixed locations, and study spatial distributions of pollutants. While analysis of individual chase events provides emission estimates for specific vehicles (Canagaratna *et al.* 2004), here we present a complementary approach which considers all measurements while the laboratory is driving throughout the city as potential vehicle exhaust plumes. The objectives of this research are to develop a method that can be used to estimate fleet-average emissions from data collected by a mobile laboratory and then to apply this method to estimate emissions of BC, PPAHs, and gas-phase species in Mexico City. Based on the measurement of emission ratios and by carbon balance, we have characterized the distribution of emissions among the fleet and estimated the city's motor vehicle emission inventory.

## **Experimental section**

### ***Mobile laboratory***

A mobile laboratory designed and built by Aerodyne Research, Inc. (ARI, Billerica, MA) was deployed during the MCMA-2003 field campaign (Fig 1.1). It was equipped with a comprehensive suite of state-of-the-art fast response instruments for gas and particle measurements, including an aethalometer (AE-16, Magee Scientific) that measures BC, a photoelectric aerosol sensor (PAS, EcoChem PAS 2000CE) that measures particle-bound PAHs, a non-dispersive infrared (NDIR) unit (Li-Cor LI 6262) that measures carbon dioxide (CO<sub>2</sub>), an ARI tunable infrared laser differential absorption spectrometry (TILDAS) that measures carbon monoxide (CO) measurements, a chemiluminescent analyzer (Thermo 42C) that measures total nitrogen oxides (NO<sub>y</sub>), and a proton transfer

reaction mass spectrometer (PTR-MS) that measures speciated volatile organic compounds (VOCs). Some environmental parameters such as the van's speed, wind speed and direction, temperature, relative humidity and pressure were also measured by onboard instruments. Furthermore, a video camera facing forward continuously recorded the driver's view and provided visual records of the chase experiments, such as traffic conditions and types of the targeted vehicles.

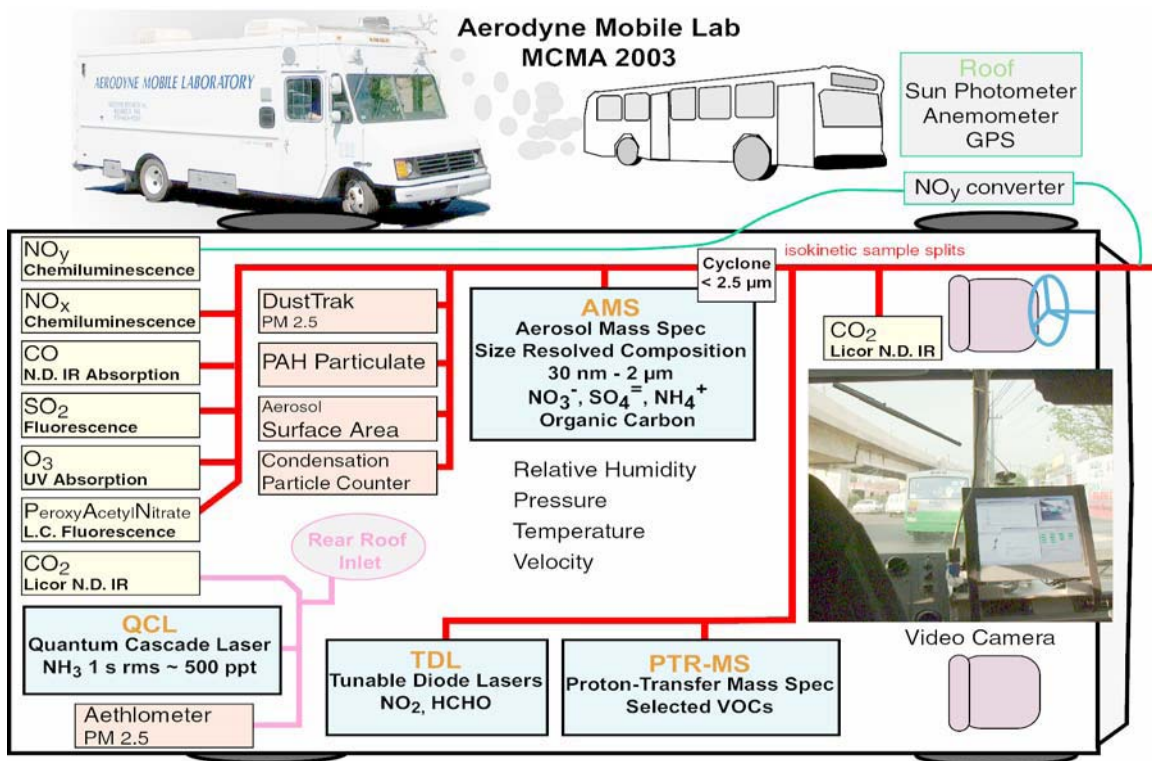


**Figure 1.1** Schematic of the ARI mobile laboratory as instrumented for the MCMA-2003 field campaign.

### *Mobile experiments*

Previous mobile lab studies have mainly focused on characterizing emissions from individual vehicles by segmenting the measurements by chase events, based on manual analysis of concentration data and video captured by the van's onboard camera. In contrast to such a microscopic approach, we instead use a macroscopic approach, where we attempt to identify many measurements representing a large number of vehicles and then to calculate fleet-average emissions. The laboratory continuously samples ambient

air from an inlet at the front of the van, and it is always “seeing” exhaust plumes from the vehicles around it while driving through traffic. That is, even when not actively chasing a particular vehicle, the mobile laboratory is still sampling fresh tailpipe exhaust from the vehicles around it. In this analysis, we considered 75 hours of data collected over 13 days of driving in all different directions from the field campaign’s base at the Universidad Autonoma de México (UAM) in Iztapalapa. As described in the following section, we analyze pollutant and meteorological measurements and video of the view in front of the lab to develop criteria for the separation of exhaust plumes from the background.

### *Data analysis*

The continuous measurements of pollutant concentrations represent three types of measurements: 1) fresh tailpipe exhaust, 2) background, and 3) exhaust directly from or contaminated by emissions from the mobile lab’s engine and generator, referred to as “self-sampling” in this paper. Our objective is to quantify emissions from on-road motor vehicles, so we consider only those data points likely to have vehicle exhaust as the sole source. Therefore, the identification and elimination of background and self-sampling measurements is an essential component of the calculation.

The identification of tailpipe exhaust and background sampling is based on the real-time concentrations of CO<sub>2</sub>, which is a direct tracer of emissions from vehicles using carbonaceous fuels. As “baseline” is defined here as the minimum ambient level of pollutant concentrations, we use the term “background measurement” to refer to those data points that are not significantly above the “baseline.” “Background” points are therefore believed to represent the ambient measurements minimally influenced by nearby vehicles, as opposed to vehicle exhaust plume measurements. The baseline will change in space and time, as it is influenced by diurnal meteorological patterns and neighborhood-scale emissions. For example, the “baseline” in a neighborhood with numerous busy roads at a stagnant time of day will be higher than in a large park during a windy period.

The baseline is constructed by setting the fifth lowest value in a moving time window of 3 minutes as the baseline value of all corresponding data points for the 180 seconds. We

tested window widths ranging from 1 to 15 minutes and found that a width of 3 minutes best balanced short and long-term variability in the baseline. We selected the 5th lowest value in every time window, rather than the lowest one, to account for outliers.

To determine a criterion to separate background from exhaust plume measurements, we analyzed the CO<sub>2</sub> measurements during the time periods when the van was parked away from traffic to find the natural variance of ambient CO<sub>2</sub> concentrations. We found that 95% of the data points lie within 42 ppm above the baseline. Therefore, we defined “42 ppm above baseline” as a threshold for potential exhaust plumes (Fig 1.2). Any points that exceed the threshold are considered exhaust plume measurements; those that fall below the threshold are considered background measurements.

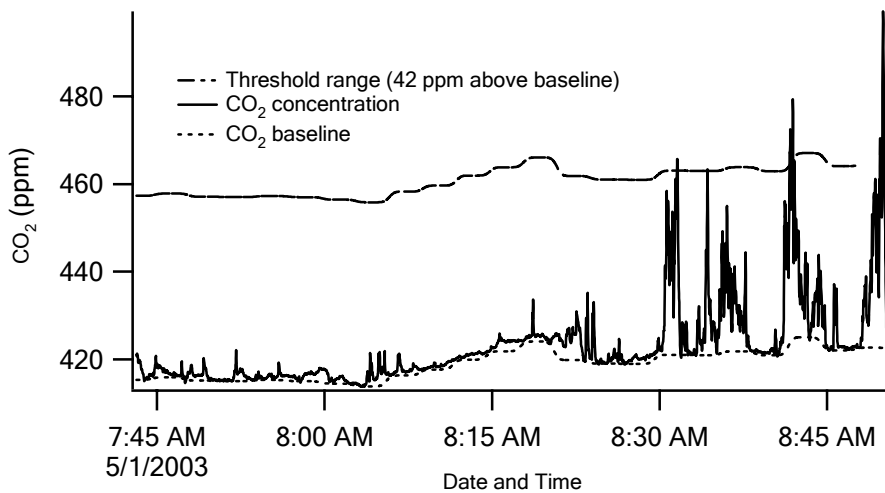


**Figure 1.2** Determination of the natural background variance of CO<sub>2</sub> concentrations based on measurements while the mobile lab was parked. If a data point indicating a concentration above the natural background threshold range is detected, the point is considered a potential exhaust plume measurement.

“Self-sampling” is defined as sampling of air parcels that are contaminated by emissions from the onboard generator and the mobile lab’s own tailpipe. The generator was found to emit methanol, which is not common in the exhaust of Mexico City’s vehicle fleet and is therefore used as a tracer to identify self-sampling of the generator (Fig 1.3). Furthermore, the wind direction relative to the sampling inlet is also indicative of self-sampling. When the wind comes from behind the van or the driver’s side where the van’s

tailpipe and its onboard generator are located, the corresponding measurements are likely to be influenced by emissions from these two outlets. In fact, when the wind direction is in the range of 180-300 degrees (Figs 1.3, 1.4), elevated methanol concentrations are often found, indicating self-sampling. We extend the self-sampling wind direction range to 90-300 degrees to eliminate potential sampling of the mobile lab's own tailpipe emissions. Overall, approximately 40% of points are identified as self-sampling measurements.

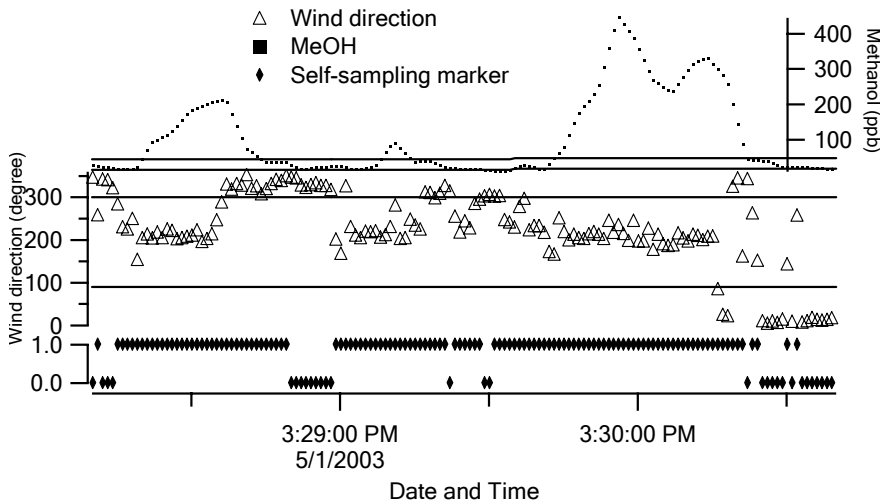


**Figure 1.3** Self-sampling identification: points with methanol concentrations (from the generator's exhaust) more than 30 ppb above the baseline (upper section), and wind directions between 90 and 300 degrees (middle section), are labeled as self-sampling, indicated by the self-sampling marker time series (lower section). In the marker time series, a value of 1 indicates self-sampling, and 0 indicates absence of self-sampling.

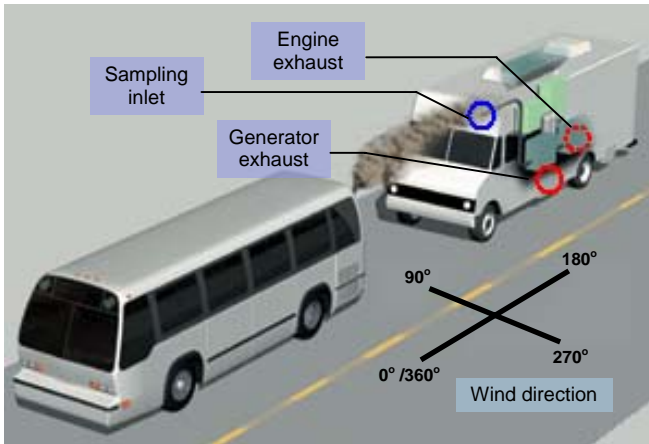


**Figure 1.4** Location of the sampling inlet, van’s onboard generator and its own tailpipe (rear). Measurements made when wind originates between 90 and 300 degrees are considered to be contaminated by the van’s generator and engine exhaust.

Upon identification of potential exhaust plume and self-sampling measurements, we construct a time series of markers that labels each one-second data point as one of three types (Fig 1.5): 1 for valid exhaust measurements, 0 for background measurements, and -1 for self-sampling. This time series, based on CO<sub>2</sub>, wind direction, and methanol, is then applied universally to any other pollutant time series, e.g. CO, BC, PPAHs, to identify exhaust measurements.

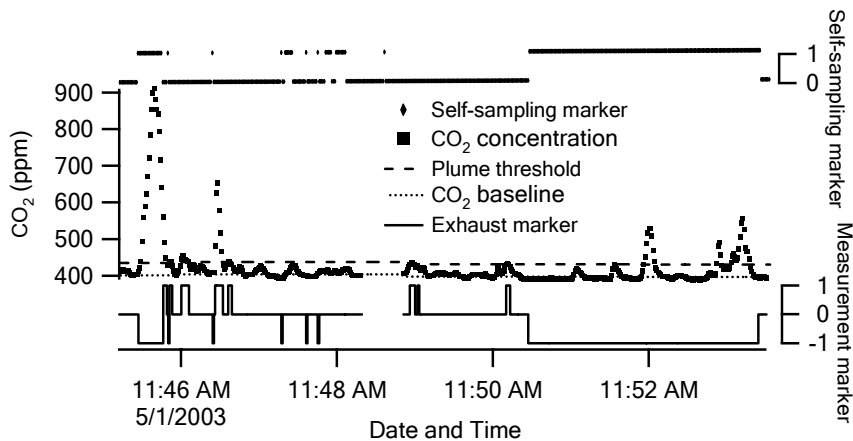


**Figure 1.5** Construction of the exhaust measurement marker time series: those points that are marked as self-sampling in the self-sampling marker time series (value of 1) are labeled with -1 in the exhaust marker time series. Those that lie below the background threshold range are labeled with 0 as background measurements; the rest are labeled with 1 as exhaust plume measurements.

### ***Emission factors***

By performing a carbon balance on the fuel combustion process, one can relate the emissions of carbon-containing species in vehicle exhaust to fuel consumption. If  $[C_f]$  refers to the carbon content originally in the fuel,  $[CO_2]$ ,  $[CO]$ ,  $[VOC]$ ,  $[BC]$  and  $[PPAH]$  represent the carbonaceous species produced during combustion, and  $[C_0]$  accounts for all remaining carbon-containing species, such as fuel residues and other non-volatile organic compounds, the following mass balance should be observed:

$$[C_f] = [CO_2] + [CO] + [VOC] + [BC] + [PPAH] + [C_0] \quad (1)$$

Considering that the sum of BC, PPAHS and  $C_0$  are very likely to be less than 0.1% of  $C_f$  (Hansen *et al.* 1990), we simplify the equation to:

$$[C_f] = [CO_2] + [CO] + [VOC] \quad (2)$$

Therefore, the fuel-based emission factor can be calculated using the following equation:

$$E_p = \frac{\Delta[P]}{\Delta[CO_2] + \Delta[CO] + \Delta[VOC]} w_c \quad (3)$$

where  $E_p$  is the emission factor of pollutant P in grams of pollutant emitted per kg of fuel consumed;  $\Delta[P]$  is the concentration of pollutant P above the baseline value, expressed in grams per cubic meter of air;  $\Delta[CO_2]$ ,  $\Delta[CO]$  and  $\Delta[VOC]$  are the concentration increases of  $CO_2$ , CO and VOC above their baseline values, expressed in grams of carbon per cubic meter of air; and  $w_c$  is the mass fraction of carbon in the fuel. In this work, we compute the emission factors for the pollutants BC, PPAHs, CO, benzene, total VOC and  $NO_y$ . Due to the slower response times of some instruments (BC, CO and PPAH), we integrate concentrations over 10-second periods. The integration did not produce significantly different results even for instruments with true 1-second response times.

### ***Emission inventory***

By multiplying the annual fuel sales in Mexico City by the emission factors, we can estimate the emission inventory, or total emissions for each pollutant species. The area's

fuel sales data were initially obtained as 6.90 and 1.62 billion liters per year for gasoline and diesel, respectively, in the year 2000 (CAM 2001). We use an average fuel density of 760 g L<sup>-1</sup> fuel and carbon content of 0.85, based on an average of gasoline and diesel fuel properties (Delucchi et al. 2003) weighted by the volume of sales of each.

## Results

**Table 1.1** Emission factors of the measured pollutants from on-road motor vehicles in Mexico City (MCMA-2003)

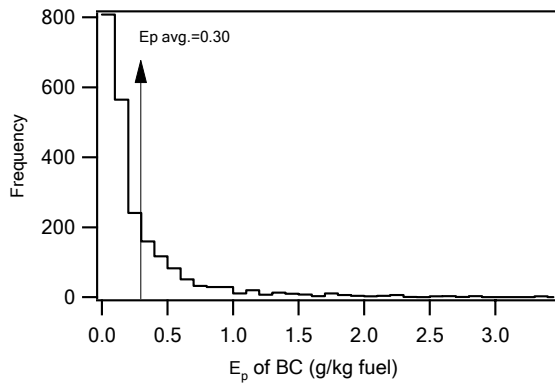
g kg <sup>-1</sup> fuel	$\bar{x}$	s <sub>x</sub>
BC	0.301	0.483
PPAHs	0.00862	0.0102
CO	204	178
Benzene <sup>a</sup>	0.661	0.376
VOCs <sup>a</sup>	35.4	20.2
NO <sub>y</sub> <sup>b</sup>	19.1	12.4

<sup>a</sup>. Benzene was measured in real time by a proton transfer reaction and mass spectrometry (PTR-MS). The emission factor of benzene is used in this study to estimate total VOCs with a total VOC/benzene ratio obtained from measurements of speciated VOCs in morning time ambient air in Mexico City (Lamb 2004).

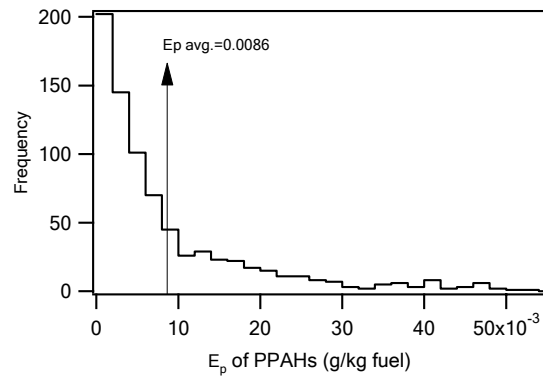
<sup>b</sup>. NO<sub>y</sub> is reported as NO<sub>2</sub> in terms of mass.

Table 1.1 summarizes the emission factors for each species. Benzene is used as a surrogate for VOCs because fast measurements of total VOCs are not available with the mobile lab. From canister-based speciated VOC measurements collected during the morning hours, when vehicle emissions are dominant and fresh, the VOC/benzene ratio is 53.6 by mass (Lamb *et al.* 2004). We then apply this ratio to the results for benzene to estimate VOC emissions. As shown in the table, CO and VOCs have the highest emission factors among the carbonaceous species, representing about 24% and 4% respectively of carbon in the exhaust, while BC and PPAHs rank among the lowest emission factors and account for about 0.04% and less than 0.001% of carbon in the exhaust, which is consistent with our earlier assumption for the simplified mass balance. Also note that the standard deviations (s<sub>x</sub>) are generally large because of the skewed distributions, but the large number of measurements (~3,600 valid 10-second periods) results in a much smaller standard error and narrower confidence interval.

The distributions of the emission factors for different species are illustrated with histograms in Figures 1.6-1.10. Those species with a near-zero mode, such as BC and PPAHs, are dramatically skewed by a small number of high value points, while species like  $\text{NO}_y$  and benzene are more normally distributed. The implications of the different distribution patterns will be discussed in the following section.



**Figure 1.6** Histogram of BC emission factors.



**Figure 1.7** Histogram of PPAH emission factors.

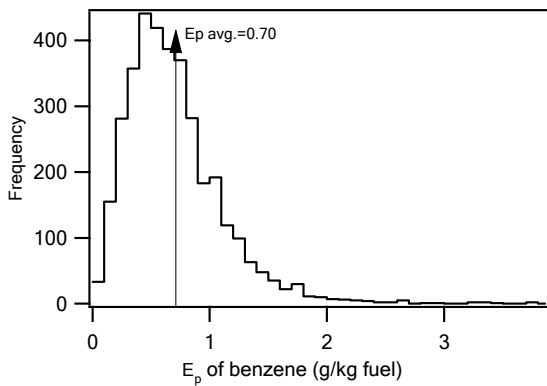


**Figure 1.8** Histogram of benzene emission factors.

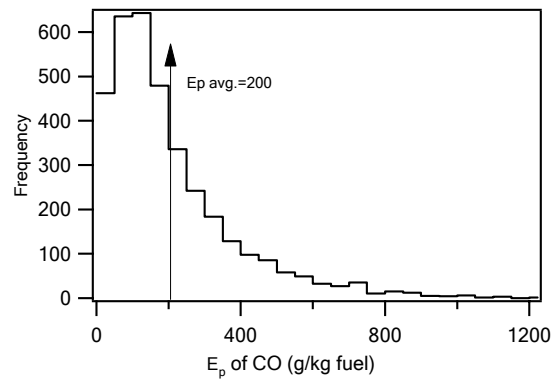


**Figure 1.9** Histogram of CO emission factors.

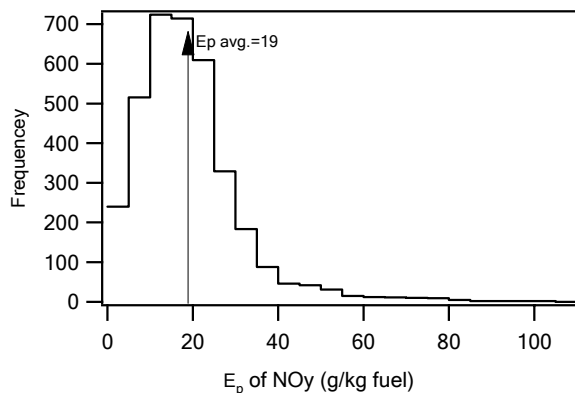


**Figure 1.10** Histogram of  $\text{NO}_y$  emission factors.

## Discussion

As shown in the histograms of the emission factors, the distributions of the emission factors are skewed to different degrees. The skewness coefficient of black carbon, as an extreme example, is 5.7; and that of the other species is less than 2.0 in all cases. The skewness may indicate the degree to which a pollutant is mainly emitted by certain types of vehicles that make up a small fraction of the fleet. BC is expected to be emitted mainly by diesel vehicles, while the other pollutants are also emitted by gasoline-powered vehicles, which make up the majority of the fleet. The few data points with very high ratios considerably affect the means for some of the species such as BC, PPAHs and CO. The discrepancy between the mean and the mode illustrates how a relatively very small number of “super polluters” raise the average emission factor. In fact, if the highest 20% of the points are eliminated, the average emission factors can be reduced by half, respectively 54% and 50% for BC and PPAHs, which corresponds to comparable reductions in the total emissions. On the other hand, species like  $\text{NO}_y$  and benzene are not skewed as much by the “super polluters” as the BC and PPAHs. Eliminating the highest 20% of values will only result in a 24% and 23% reduction in their emission factors, respectively. With a moderate skewness level, CO receives a reduction of 36% to the emission factor with the highest 20% points removed. These distribution patterns suggest that policies like replacing a portion of the oldest vehicles, which only targets the “super polluters”, will have the greatest effect on BC and PPAH emissions and less of an effect on  $\text{NO}_y$  and benzene (or VOCs).

We compared our results for the gas-phase pollutants to the Metropolitan Environmental Commission's (CAM) estimates for the year 2000, the most recent year for which the emission inventory is available. The government agency has been making the estimates for several years since 1996 using a customized version of the U.S. Environmental Protection Agency's MOBILE model, and seeks confirmation of its results by other methods. The comparisons in general suggest good agreement, which adds confidence to both estimates (Fig 1.11, Table 1.2). The 34% and 20% differences between the two estimates for CO and NO<sub>y</sub> respectively, indicate that the vehicle emissions of the two pollutants may have been significantly reduced over the period between year 2000 and 2003 due to the progressing measures to control vehicle emissions taking place in the city, such as use of reformulated fuels and the enforcement of a vehicle inspection and maintenance program. On the other hand, when the estimates of total emission based on the emission factors measured in 2003 are generally expected to be lower than that in 2000, our estimate of VOC total emission is 18% higher than that made by the government previously. In fact, it was suggested that the emission inventory models often underestimate VOC and CO emissions (Sawyer *et al.* 1998, Arriaga-Colina *et al.* 2004). Also, using the ambient VOC/benzene ratio to estimate vehicle source emissions of VOCs contributes uncertainty, as other sources may add to the total VOC and benzene concentrations and may have different VOC/benzene ratios. This uncertainty can be determined in the future when fast measurement of total VOCs become available in the mobile laboratory. An additional source of uncertainty stems from the fact that cold-start emissions are not captured during mobile lab experiments and are therefore not included in our emission estimates.

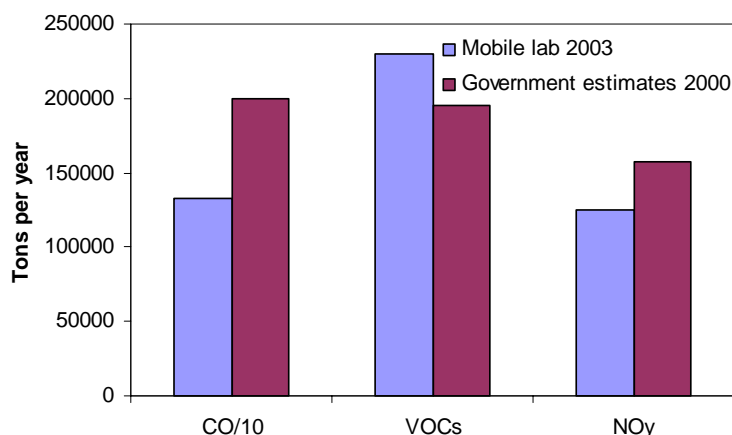


**Figure 1.11** Comparison of annual emissions of CO, NO<sub>y</sub> and VOCs using the new mobile lab-based method for the year 2003 versus government estimates for the year 2000.

**Table 1.2** Comparison of emission inventories based on the mobile laboratory measurements in spring 2003, government modeling estimates of Mexico City in 2000 and ambient pollutant to CO<sub>2</sub> ratios measured during MCMA-2003.

(tons y <sup>-1</sup> )	This study <sup>b</sup>	Government estimate	Alternative approach <sup>a</sup>
BC	1,960 ± 130		2,500 ± 720
PPAHs	56.2 ± 4.7		29.7 ± 8.6
CO	1,330,000 ± 380,000	2,000,000	
VOC	230,000 ± 4,000	195,000	
NO <sub>y</sub>	125,000 ± 3,000	157,000	

<sup>a</sup>. The government does not estimate BC or PPAH emissions. Instead, we multiplied the  $\Delta [P]/\Delta [CO]$  ratio, which is obtained from ambient measurements at Universidad Autónoma Metropolitana (UAM), the supersite of the field campaign, during MCMA-2003, and the total emissions of CO in Mexico City. The lower limit uses the government estimate of CO emissions, and the upper limit uses the estimate determined in this study.

<sup>b</sup>. Mean ± 1.96 standard error (95% confidence interval).

We also compared our estimates for the total emissions of black carbon and PPAHs to the results acquired from an alternative approach, in which the ambient BC/CO and PPAHs/CO ratios are multiplied by the total vehicle source CO emissions in the city (Table 1.2). The ratio of BC/CO was found to be  $1.63 \mu\text{g m}^{-3} \text{ppm}^{-1}$  ( $R^2 = 0.64$ ) during the MCMA-2003 field campaign, measured at the supersite at UAM in Iztapalapa. This alternative estimate is about 28% higher than our fuel-based result, which is consistent with the common understanding that the ambient measurements also detect BC emissions

from sources other than on-road motor vehicles. Likewise, the ambient PPAHs/CO ratio was found to be  $19.3 \text{ ng m}^{-3} \text{ ppm}^{-1}$  ( $R^2 = 0.71$ ), but the alternative estimate is ~50% lower than the result from the mobile lab. We believe the reason for this is largely due to the particle aging or coating that occurs during the transport from vehicle tailpipes to ambient monitoring site, and a large portion of the surface adsorbed PAHs becomes no longer detectable by the photoelectric aerosol sensor, which only measures PAHs on the particle surfaces.

Table 1.3 lists the values of emission factors of BC and/or PPAHs determined in some previous studies. There seems also to be reasonable agreement between these previous results and our calculated BC and PAH emission factors.

**Table 1.3** Emission factors of BC and PPAHs for gasoline and diesel, or light-duty and heavy-duty vehicles, determined in tunnel experiments and remote sensing studies.

Reference	Method	BC $\text{g kg}^{-1}$ fuel	PPAHs $\text{g kg}^{-1}$ fuel
Hansen <i>et al.</i> (1985)	Remote sensing	0.0034 - 0.85	N/A
Weingartner <i>et al.</i> (1996)	Tunnel study	Diesel: 0.48 <sup>a</sup>	0.013 <sup>a</sup>
Miguel <i>et al.</i> (1998)	Tunnel study	LDV: $0.030 \pm 0.002$ HDV: $1.44 \pm 0.16$	LDV: $8.85 \times 10^{-5}$ <sup>b</sup> HDV: $1.40 \times 10^{-3}$
Marr <i>et al.</i> (1999)	Tunnel study	N/A	LDV: $9.04 \times 10^{-5}$ <sup>b</sup> HDV: $2.33 \times 10^{-3}$
Kirchstetter <i>et al.</i> (1999)	Tunnel study	LDV: $0.035 \pm 0.003$ HDV: $0.13 \pm 0.3$	N/A
This study	Mobile lab	Combined: 0.30	0.0086

<sup>a</sup>. Assuming an average fuel economy of 10 mpg according to the vehicle composition in the experiment.

<sup>b</sup>. This emission factor is the sum of 10 individual PAHs.

This method is potentially biased by the fact that the number of data points representing different types of vehicles that were chased and sampled may be disproportional to the actual distribution of the vehicle types in the city. But it is reasonable to assume that the probability of measuring a certain vehicle type would be relatively consistent with the percentage of this specific type of vehicles in the city's fleet. It is also reasonable to assume that large plumes, which are sampled at a higher rate, should receive higher weight when considering such vehicles' contribution to total emissions. Additionally, to

account for self-sampling by the mobile lab, we have excluded points containing methanol, but we may have inadvertently screened out other vehicles' exhaust that contains methanol. At this point in time, such vehicles, mainly methanol-powered ones, are not expected to contribute significantly to Mexico City's motor vehicle emission inventory. A final source of uncertainty stems from compositing fuel properties, i.e. carbon weight fraction and density, for use in Eq. 3 and emission inventory calculations. Carbon weight fractions differ by only 2% between gasoline and diesel fuel, but their densities differ by 13%. Our use of a sales-weighted density should minimize error.

The advantage of this method is its ability to provide a comprehensive estimate of mobile source emission inventories, taking into consideration of a variety of types of vehicle under the full range of real-world driving conditions. In future work, we suggest using additional statistical analyses to try to identify the different types of engines associated with each exhaust plume point. Principal component analysis could be used to study the expected covariance between, for example, high  $\text{NO}_y$  and high BC emissions that might be associated with diesel vehicles.

## **Conclusions**

We have used a mobile lab to measure motor vehicle emissions of BC, PPAHs, and gaseous species in Mexico City. To calculate a fuel-based emission inventory, we developed an algorithm that automatically identifies exhaust plume measurements. Out of 75 hours of sampling, the method has identified ~3,600 data points (with 10 sec time resolution) corresponding to exhaust plumes. Motor vehicles are estimated to emit annually  $1,960 \pm 130$  tons BC,  $56.2 \pm 4.7$  tons PPAHs,  $1,330,000 \pm 380,000$  tons CO,  $125,000 \pm 3,000$  tons  $\text{NO}_y$  and  $2300 \pm 4,000$  tons VOCs. The distributions of the emission factors are found to be skewed to varying degrees. As a result, the total emissions of BC and PPAHs can be reduced by approximately 50% if the top 20% data points with the highest ratios are removed, but the "super polluters" are less influential on  $\text{NO}_y$  and benzene emissions. Mobile measurement of total VOCs is desired in order to more directly estimate VOC emissions from vehicle sources using this method. This method can be combined with manual analysis of chase events, so that the emissions of

individual vehicles or vehicle classes can be studied while self-sampling and background measurements are conveniently detected and separated from those of the real exhaust plumes.

### **Acknowledgements**

This research was supported by funds from the Alliance for Global Sustainability and the Mexican Metropolitan Environmental Commission to the Integrated Program on Urban, Regional and Global Air Pollution at MIT. We are also grateful to Aerodyne Research Inc. and other participants in MCMA-2003 field campaign.

### **References**

Arriaga-Colina, J. L., West, J.J., Sosa, G., Escolona, S.S., Ordunez, R.M., Cervantes, A.D.M. (2004). "Measurements of VOCs in Mexico City (1992-2001) and evaluation of VOCs and CO in the emissions inventory." *Atmospheric Environment* **38**(2004): 2523-2533.

ATSDR (1995). Toxicological Profile for Polycyclic Aromatic Hydrocarbons, Agency for Toxic Substances and Disease Registry.

CAM, Mexico Metropolitan Environmental Commission (2001). "Inventario de Emisiones 1998 de la Zona Metropolitana del Valle Mexico, Version Preliminar."

Canagaratna, M. R., Jayne, J.T., Ghertner, D.A., Herndon, S., Shi Q., Jimenez, J.L., Silva, P.J., Williams, P., Lanni, T., Drewnick, F., Demerjian, K.L., Kolb, C.E., Worsnop, D.R. (2004). "Chase studies of particulate emissions from in-use New York City vehicles." *Aerosol Science and Technology* **38**(6): 555-573.

Delucchi, M. A. (2003). A lifecycle emissions model (LEM): lifecycle emissions from transportation fuels, motor vehicles, transportation modes, electricity use, heating and cooking fuels, and materials, Institute of Transportation Studies, UC Davis.

Denissenko, M. F., Pao, A., Tang, M.S., Pfeiffer, G.P., (1996). "Preferential formation of benzo[a]pyrene adducts at lung cancer mutational hotspots in P53." *Science* **274**(5286): 430-432.

Finlayson-Pitts, B. J., Pitts, J.N. (2000). *Chemistry of the Upper and Lower Atmosphere*. San Diego, Academic Press.

Hansen, A. D. A., Rosen, H., (1990). "Individual Measurements of the Emission Factor of Aerosol Black Carbon in Automobile Plumes." *Air Waste Manage, Assoc.* **40**: 1654-1657.

Jacobson, M. Z. (2002). "Control of fossil-fuel particulate black carbon and organic matter, possibly the most effective method of slowing global warming." *Journal of Geophysical Research - Atmospheres* **107**(D19): Art. No. 4410.

Kolb, C. E. H., S. C.; Mcmanus, J. B.; Shorter, J. H.; Zahniser, M. S.; Nelson, D. D.; Jayne, J. T.; Canagaratna, M. R.; Worsnop, D. R. (2004). "Mobile Laboratory with Rapid Response Instruments for Real-Time Measurements of Urban and Regional Trace Gas and Particulate Distributions and Emission Source Characteristics." *Environmental Science and Technology* **38**(21): 5694-5703.

Lamb, B., Velasco, E., Allwine, E., Westberg, H., Herndon, S., Knighton, B., Grimsrud, E., (2004). Ambient VOC Measurements in Mexico City. (manuscript)

Lobscheid, A. B., McKone, T.E., (2004). "Constraining uncertainties about the sources and magnitude of polycyclic aromatic hydrocarbon (PAH) levels in ambient air: the state of Minnesota as a case study." *Atmospheric Environment* **38**(33): 5501-5515.

Molina, L. T., Molina, M.J., (2002). *Air Quality in the Mexico Megacity: An Integrated Assessment*. Boston, Kluwer Academic Publishers.

Molina, L. T., Molina, M.J., (2004). "Improving Air Quality in Megacities: Mexico City Case Study." *Annals of the New York Academy of Sciences* **1023**(142-158).

Sawyer, R.F., Harley, R.A., Cadle, S.H., Norbeck, J.M., Slott, R., Bravo, H.A., (1998). "Mobile sources critical review: 1998 NARSTO assessment." *Atmospheric Environment* **34**(2000): 2161-2181.

USEPA (1995). Contaminant Specific Fact Sheets, National Primary Drinking Water Regulations (NPDWR). **Title 40, Volume 19**.

## Appendix A

### Emission Inventory Calculations

#### 1. Emission Factor

##### 1.1 Mass Balance

By performing a carbon balance on the fuel combustion process, one can relate the emissions of carbon-containing species in vehicle exhaust to fuel consumption. If  $[C_f]$  refers to the carbon content originally in the fuel,  $[CO_2]$ ,  $[CO]$ ,  $[VOC]$ ,  $[BC]$  and  $[PPAH]$  are the carbon-containing combustion products, and  $[C_0]$  represents all the remaining carbon-containing species in the exhaust, such as fuel residues and other non-volatile organic compounds, all expressed in grams of carbon per kg fuel consumed, then the following mass balance will be observed:

$$[C_f] = [CO_2] + [CO] + [VOC] + [BC] + [PPAH] + [C_0] \quad (1)$$

Knowing that the sum of BC, PPAH and  $C_0$  are very likely to be extremely small portions of  $C_f$ , we simplify the equation to:

$$[C_f] = [CO_2] + [CO] + [VOC] \quad (2)$$

Therefore, the fuel-based emission factor  $E_p$ , in units of grams of pollutant emitted per kg of fuel burned, can be calculated using the following equation:

$$E_p = \frac{\Delta[P]}{\Delta[CO_2]f_{CO_2} + \Delta[CO]f_{CO} + \Delta[VOC]f_{VOC}} w_c \quad (3)$$

where  $\Delta[P]$ ,  $\Delta[CO_2]$ ,  $\Delta[CO]$  and  $\Delta[VOC]$  are the concentration increases of pollutant P,  $CO_2$ , CO and VOC above their baseline values, expressed in grams of pollutants per cubic meter of air. The terms  $f_{CO_2}$ ,  $f_{CO}$  and  $f_{VOC}$  are mass fraction of carbon in these pollutants, expressed in gram of carbon per ppm of pollutant. The term  $w_c$  is the mass fraction of carbon in the fuel, expressed in grams of carbon per kg of fuel. In this work, we compute the emission factors for the pollutants BC, PPAHs, CO, VOCs and  $NO_y$ .

## 1.2 Calculations

Constant values:

Atmospheric pressure	P	0.75 atm
Temperature	T	298 K
Molecular weight	MW <sub>CO<sub>2</sub></sub>	12 g mol <sup>-1</sup>
Fuel density	ρ <sub>f</sub>	760 g L <sup>-1</sup> fuel
Carbon content in fuel	w <sub>c</sub>	850 g C kg <sup>-1</sup> fuel
VOC-benzene volume ratio	$\frac{V_{\text{VOC}}}{V_{\text{benzene}}}$	97.5 ppm ppm <sup>-1</sup> †
Carbon number in average VOC molecular formula		3.12 <sup>†</sup>
VOC-benzene mass ratio	$\frac{m_{\text{VOC}}}{m_{\text{benzene}}}$	53.6 g g <sup>-1</sup> †

† These are estimated based on the speciation of VOCs in the early-morning ambient measurements during the MCMA-2003 field campaign (Lamb 2004).

Equation 3 can be rearranged to:

$$E_p = \frac{\frac{\Delta[P]}{\Delta[\text{CO}_2]}}{f_{\text{CO}_2} + \frac{\Delta[\text{CO}]}{\Delta[\text{CO}_2]} f_{\text{CO}} + \frac{\Delta[\text{VOC}]}{\Delta[\text{CO}_2]} f_{\text{VOC}}} w_c \quad (4)$$

We calculate the emission factors using pollutant/CO<sub>2</sub> ratios to maintain consistency with other work using the Aerodyne mobile laboratory and to facilitate common analyses.

**Table A.1** ΔP/ΔCO<sub>2</sub> ratios of different pollutants for one data point

	$\bar{x}$	units
ΔBC/ΔCO <sub>2</sub>	0.229	μg ppm <sup>-1</sup> CO <sub>2</sub>
ΔPPAHs/ΔCO <sub>2</sub>	5.02	ng ppm <sup>-1</sup> CO <sub>2</sub>
ΔCO/ΔCO <sub>2</sub>	0.149	ppm ppm <sup>-1</sup> CO <sub>2</sub>
ΔBenzene/ΔCO <sub>2</sub>	0.124	ppb ppm <sup>-1</sup> CO <sub>2</sub>
ΔNO <sub>y</sub> /ΔCO <sub>2</sub>	8.15	ppb ppm <sup>-1</sup> CO <sub>2</sub>

Table A.1 presents pollutant/CO<sub>2</sub> ratios for one data point as an example. To calculate the denominator in Equation 4, we first need to convert  $\Delta\text{benzene}/\Delta\text{CO}_2$  to  $\Delta\text{VOC}/\Delta\text{CO}_2$ :

$$\frac{\Delta[\text{VOC}]}{\Delta[\text{CO}_2]} = \frac{\Delta[\text{benzene}]}{\Delta[\text{CO}_2]} \frac{V_{\text{VOC}}}{V_{\text{benzene}}} = \frac{0.124 \times 10^{-3} \text{ ppm benzene}}{\text{ppm CO}_2} \times \frac{97.5 \text{ ppm VOC}}{\text{ppm benzene}} = 1.21 \times 10^{-2} \text{ ppm VOC}$$

and

$$f_{\text{CO}_2} = \frac{(0.750 \text{ atm})(10^{-6})}{(82.06 \times 10^{-6})(298\text{K})} 12 \text{ g C/mol CO}_2 = 3.68 \times 10^{-4} \text{ g C ppm}^{-1} \text{ CO}_2$$

$$f_{\text{CO}} = \frac{(0.750 \text{ atm})(10^{-6})}{(82.06 \times 10^{-6})(298\text{K})} 12 \text{ g C/mol CO} = 3.68 \times 10^{-4} \text{ g C ppm}^{-1} \text{ CO}$$

$$f_{\text{CO}_2} = \frac{(0.750 \text{ atm})(10^{-6})}{(82.06 \times 10^{-6})(298\text{K})} 3.12 \times 12 \text{ g C/mol CO}_2 = 1.15 \times 10^{-3} \text{ g C ppm}^{-1} \text{ VOC}$$

Therefore, part of the denominator in Equation 3 is:

$$\begin{aligned} f_{\text{CO}_2} + \frac{\Delta[\text{CO}]}{\Delta[\text{CO}_2]} f_{\text{CO}} + \frac{\Delta[\text{VOC}]}{\Delta[\text{CO}_2]} f_{\text{VOC}} &= 3.68 \times 10^{-4} + 0.149(3.68 \times 10^{-4}) + (1.21 \times 10^{-2})(1.15 \times 10^{-3}) \\ &= 4.92 \times 10^{-4} \text{ g C ppm}^{-1} \text{ CO}_2 \end{aligned}$$

So, we now can calculate the emission factors as following:

$$E_{\text{BC}} = \frac{0.229 \times 10^{-6} \text{ g / ppmCO}_2}{4.92 \times 10^{-4} \text{ g C/ppm CO}_2} \frac{850 \text{ g C}}{\text{kg fuel}} = 0.396 \text{ g BC kg}^{-1} \text{ fuel}$$

$$E_{\text{PPAHs}} = \frac{5.02 \times 10^{-9} \text{ g / ppm CO}_2}{4.92 \times 10^{-4} \text{ g C/ppm CO}_2} \frac{850 \text{ g C}}{\text{kg fuel}} = 0.00867 \text{ g PPAHs kg}^{-1} \text{ fuel}$$

$$E_{\text{CO}} = \frac{0.149 \text{ ppm CO/ppm CO}_2}{4.92 \times 10^{-4} \text{ g C/ppm CO}_2} \frac{850 \text{ g C}}{\text{kg fuel}} \frac{28 \text{ g}}{\text{mol CO}} \frac{3.07 \times 10^{-5} \text{ mol}}{\text{ppm}} = 221 \text{ g CO kg}^{-1} \text{ fuel}$$

$$\begin{aligned} E_{\text{benzene}} &= \frac{0.124 \times 10^{-3} \text{ ppm benzene/ppm CO}_2}{4.92 \times 10^{-4} \text{ g C/ppm CO}_2} \frac{850 \text{ g C}}{\text{kg fuel}} \frac{78 \text{ g}}{\text{mol benzene}} \frac{3.07 \times 10^{-5} \text{ mol}}{\text{ppm}} \\ &= 0.513 \text{ g benzene kg}^{-1} \text{ fuel} \end{aligned}$$

$$E_{\text{VOC}} = E_{\text{benzene}} \frac{m_{\text{VOC}}}{m_{\text{benzene}}} = (0.513 \text{ g benzene / kg fuel}) (53.6) = 27.5 \text{ g VOC L}^{-1} \text{ fuel}$$

$$E_{\text{VOC}} = \frac{1.21 \times 10^{-2} \text{ ppm VOC/ppm CO}_2}{4.92 \times 10^{-4} \text{ g C/ppm CO}_2} \frac{850 \text{ g C}}{\text{kg fuel}} \frac{3.12 \times 12 \text{ g C}}{\text{mol VOC}} \frac{3.07 \times 10^{-5} \text{ mol}}{\text{ppm}}$$

$$= 23.8 \text{ g VOC - C kg}^{-1} \text{ fuel}$$

Note: The ratio of VOC-C to VOC is 0.865, which yields a C/H ratio of 1:1.9, assuming 3.12C per VOC molecule, as estimated using the ambient measurements. This is very close to the generally accepted VOC formula, CH<sub>1.8</sub>.

$$E_{\text{NO}_y} = \frac{8.15 \times 10^{-3} \text{ ppm NO}_y/\text{ppm CO}_2}{4.92 \times 10^{-4} \text{ g C/ppm CO}_2} \frac{46 \text{ g}}{\text{mol NO}_2} \frac{3.07 \times 10^{-5} \text{ mol}}{\text{ppm NO}_y} \frac{850 \text{ g C}}{\text{kg fuel}}$$

$$= 19.9 \text{ g NO}_2 \text{ kg}^{-1} \text{ fuel}$$

Table A.2 below presents the statistical results of emission factors for the pollutants emitted from Mexico City's vehicle fleet.

**Table A.2** Average emission factors in Mexico City's fleet

g kg <sup>-1</sup> fuel	$\bar{x}$	$s_x^a$	Number of points
BC	0.300	0.482	2236
PPAHs	$8.62 \times 10^{-3}$	$10.2 \times 10^{-3}$	775
CO	$2.03 \times 10^2$	$1.78 \times 10^2$	3578
Benzene	0.698	0.413	3578
VOCs <sup>b</sup>	37.4	22.2	3578
NO <sub>y</sub> <sup>c</sup>	19.1	12.4	3595

<sup>a</sup>  $s_x$ : Standard deviation

<sup>b</sup> We found the mass ratio of VOC/benzene to be 53.6 g VOC/g benzene, so the standard deviation and standard error of mean for VOC was calculated by multiplying the  $E_p$  of benzene by the mass ratio.

<sup>c</sup> Expressed as NO<sub>2</sub>

## 2. Emission inventory

Emission factors are multiplied by the annual fuel sales in 2000 to obtain total emissions in tons per year (CAM 2001).

**Table A.3** 2000 Fuel sales in Mexico City and selected fuel properties

	Fuel sales (L y <sup>-1</sup> )	Fuel density (g/L)	Carbon content (g C g <sup>-1</sup> fuel)
Gasoline	6.90 × 10 <sup>9</sup>	740	0.850
Diesel fuel	1.62 × 10 <sup>9</sup>	850	0.870

Annual total fuel consumption as gasoline:

$$(6.90 \times 10^9 \text{ L}) \times 740 \text{ g L}^{-1} + (1.62 \times 10^9 \text{ L}) \times 850 \text{ g L}^{-1} \times \frac{0.870}{0.850} = 6.52 \times 10^9 \text{ kg gasoline equivalent}$$

Example:

$$\text{Total BC emissions} = \frac{0.300 \text{ g BC}}{\text{kg fuel}} \times 6.52 \times 10^9 \text{ kg y}^{-1} = 1.96 \times 10^3 \text{ tons y}^{-1}$$

**Table A.4** Annual motor vehicle emissions in Mexico City

	Total emission (metric tons y <sup>-1</sup> )
BC	1.96 × 10 <sup>3</sup> ± 0.13 × 10 <sup>3</sup> <sup>a</sup>
PPAHs	56.2 ± 4.7
CO	1.32 × 10 <sup>6</sup> ± 0.38 × 10 <sup>6</sup>
VOC	2.44 × 10 <sup>5</sup> ± 0.05 × 10 <sup>5</sup>
NO <sub>y</sub>	1.25 × 10 <sup>5</sup> ± 0.03 × 10 <sup>5</sup>

<sup>a</sup> Results are reported with  $\bar{x} \pm s_e$ , where  $s_e$  is standard error.

## 3. Alternative approach to BC and PPAH estimation

Ambient concentrations of BC, PPAHs and CO were measured at the “supersite”, on top of the CENICA laboratory building. The average  $\Delta\text{BC}/\Delta\text{CO}$  and  $\Delta\text{PPAHs}/\Delta\text{CO}$  ratios are as follows:

$$\Delta BC/\Delta CO = 1.63 \pm 0.02 \mu\text{g m}^{-3} \text{ ppm}^{-1} (R^2 = 0.64)$$

$$\Delta \text{PPAHs}/\Delta CO = 19.3 \pm 0.2 \text{ ng/m}^3 \text{ ppm}^{-1} (R^2 = 0.71)$$

Converting the units to of grams of pollutant per gram of CO:

$$\frac{\Delta BC}{\Delta CO} = \frac{1.63 \times 10^{-6} \text{ g m}^{-3}}{\text{ppm CO}} \frac{\text{ppm CO}}{3.07 \times 10^{-5} \text{ mol } 28 \text{ g CO}} \frac{\text{mol}}{28 \text{ g CO}} = 1.90 \times 10^{-3} \text{ g BC g}^{-1} \text{ CO}$$

$$\frac{\Delta \text{PPAHs}}{\Delta CO} = \frac{1.93 \times 10^{-9} \text{ g m}^{-3}}{\text{ppm CO}} \frac{\text{ppm CO}}{3.07 \times 10^{-5} \text{ mol } 28 \text{ g CO}} \frac{\text{mol}}{28 \text{ g CO}} = 2.25 \times 10^{-3} \text{ g PPAHs g}^{-1} \text{ CO}$$

Total emissions are estimated by the multiplication of the  $\Delta P/\Delta CO$  ratios with total CO emissions,  $1.32 \times 10^6 \text{ ton year}^{-1}$  (according to our estimate):

**Table A.5** Annual BC and PPAH emissions from ambient measurements.

	Total emission (tons $\text{y}^{-1}$ )
BC	$2.50 \times 10^3 \pm 0.72 \times 10^3$ <sup>a</sup>
PPAHs	$29.7 \pm 8.6$

<sup>a</sup> Results are reported with  $\bar{x} \pm s_e$ , where  $s_e$  is standard error.

## References

CAM, Mexico Metropolitan Environmental Commission, (2001). "Inventario de Emisiones 1998 de la Zona Metropolitana del Valle Mexico, Version Preliminar."

Lamb, B., Velasco, E., Allwine, E., Westberg, H., Herndon, S., Knighton, B., Grimsrud, E., (2004). Ambient VOC Measurements in Mexico City.

## **Appendix B**

### **Analysis of the fixed-site experiments:**

#### **Spatial and temporal distribution of black carbon and PPAHs**

##### **1. Introduction**

The spatial distribution and daily variations in concentrations of pollutants within the MCMA reflect the topographical characteristics and different land uses within the area. For non-reactive species like black carbon and PPAHs, the spatial and temporal distribution can also indicate the typical direction of transport of these pollutants from source to downwind locations.

##### **2. Experimental methods**

In addition to being used for vehicle chasing experiments during the MCMA-2003 field campaign, the mobile laboratory was also employed in fixed-site experiments at four different locations: CENICA, La Merced, Pedregal and Santa Ana (Fig. 1). La Merced is a central urban area in the Mexico City; the CENICA supersite is located ~20 km southeast of the city center and is surrounded by both industrial and residential facilities; southwest of the city center, Pedregal is a suburban residential area in the prevailing downwind direction; Santa Ana is a distant (~70 km from La Merced), sparsely populated area to the southeast of MCMA, with little business and industry. For each of the locations, the mobile lab continuously monitored pollutant concentrations for at least 36 hours, in order to capture the diurnal patterns. In this section, the results of these fixed-site experiments will be presented and discussed.

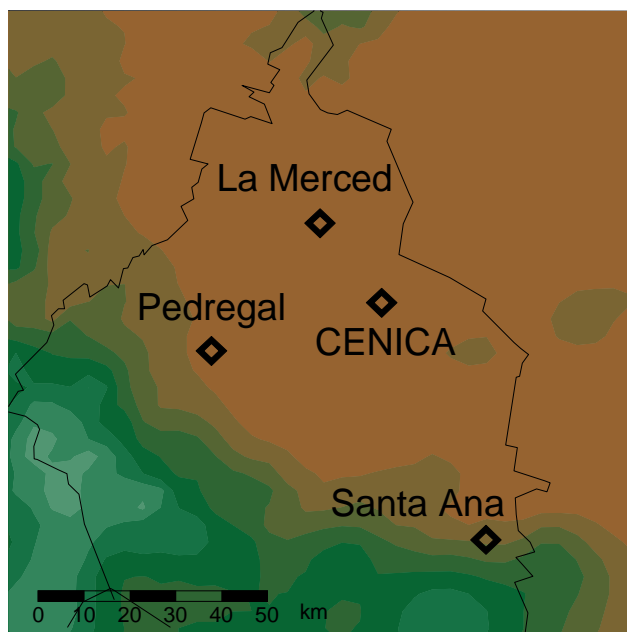


**Figure B.1** Map of the locations of the fixed-site experiments.

### 3. Results and discussion

Tables B.1 and B.2 show the typical concentrations of black carbon and PPAHS, and the hours of peak concentration at different sites in MCMA during April 2003.

**Table B.1** Typical values of 24-hr averages, daily maximum concentrations, nighttime (6 p.m. – 6 a.m.) averages and the period of time when the maximum concentrations are observed (POM) for black carbon at the four experimental sites.

	24-hr average ( $\mu\text{g m}^{-3}$ )	Daily maximum ( $\mu\text{g m}^{-3}$ )	Nighttime average ( $\mu\text{g m}^{-3}$ )	POM
La Merced	3.8	~12	2.8	6 a.m. – 11 a.m.
CENICA	1.6	~10	1.1	7 a.m. – 10 a.m.
Pedregal	2.0	~7	1.7	7 a.m. – 11 a.m.
Santa Ana	1.0	~5	1.2	9 a.m. – 9 p.m.

**Table B.2.** Typical values of 24-hr averages, daily maximum concentrations, nighttime (6 p.m. – 6 a.m.) averages and the period of time when the maximum concentrations are observed (POM) for PPAHS at the four experimental sites.

	24-hr average (ng m <sup>-3</sup> )	Daily maximum (ng m <sup>-3</sup> )	Nighttime average (ng m <sup>-3</sup> )	POM
La Merced	34	>600	30	6 a.m. – 11 a.m.
CENICA	7.0	40-80	4.4	7 a.m. – 11 a.m.
Pedregal	8.0	70-80	6.0	7 a.m. – 11 a.m.
Santa Ana	4.0	>40	3.6	6 a.m. – 9 p.m.

The highest values of black carbon and PPAHS occur in Merced (MER). Figures B.2a and B.2b clearly show that the most significant “peak period” of the day (indicated with the darker shaded areas) starts early in the morning at La Merced at about 6 a.m., the same time that traffic and street-side cooking begin in the downtown area. The concentrations start to decrease after 9 a.m., due to the end of the morning rush hour and the beginning of the growth of the boundary layer, yet they remain above the daily average until 11 a.m. The boundary layer is the lowest part of the troposphere which is directly influenced by the earth’s surface. At nighttime, it is typically shallow with a depth of a few hundreds of feet. As the sun rises and heats the surface, the boundary layer grows to 1- 3 km in depth, and this growth dilutes atmospheric pollutants in the morning.

Two other less persistent increases in black carbon and PPAH levels during the day occasionally occur around 9 - 10 p.m. and 1 - 3 a.m. (indicated with the lighter shaded areas), which may be caused by the late evening street-side cooking or garbage burning near the site, combined with the shrinkage of the boundary layer overnight. The PPAH concentration correlates very well with black carbon in terms of diurnal patterns, indicating that the two pollutants share the same source.

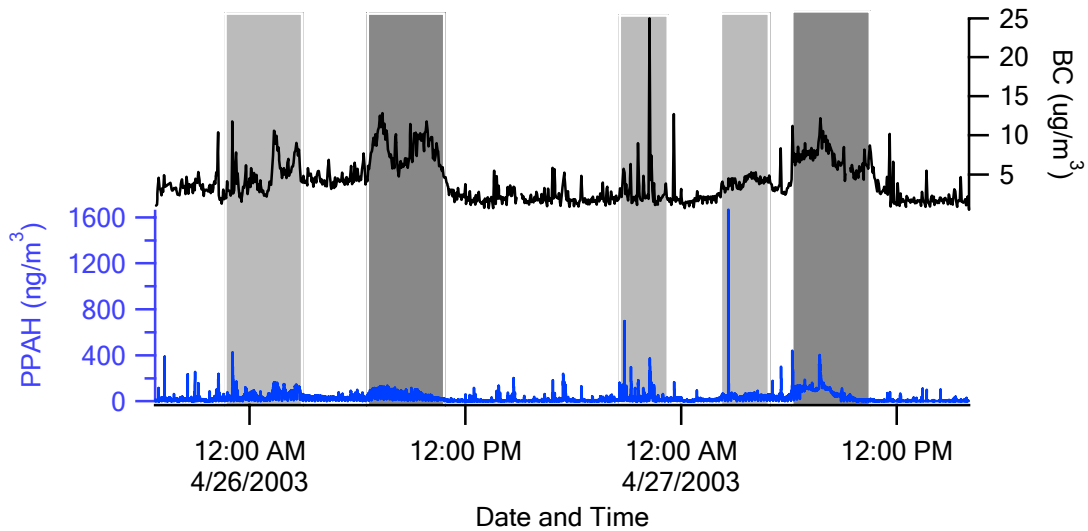


**Figure B.2a** Black carbon (BC) and PPAH concentrations measured at La Merced during the MCMA-2003 field campaign (PPAH axis shown full-scale). In this and all the following figures, peak periods are highlighted with the dark gray areas; those with the lighter gray color indicate periods of less intense or less regular increases.

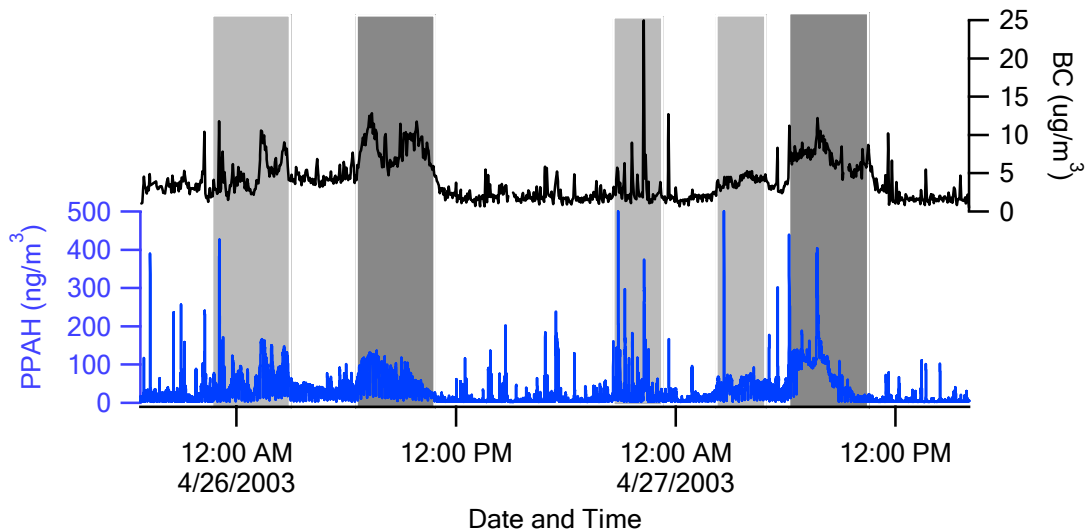


**Figure B.2b** Black carbon (BC) and PPAH concentrations measured at La Merced during the MCMA-2003 field campaign (with the PPAH axis truncated to illustrate more clearly the concentration variations).

CENICA experiences much lower concentrations of black carbon and PPAHs than in La Merced. The only period of considerably elevated concentrations during the day occurs during the morning, starting at about 7 a.m., and lasting for 2 - 4 hours (Figs. 3a, 3b). The increase begins approximately one hour later than in La Merced. The time lag between

the beginning of the peak hours observed here and in La Merced very likely results from the time needed for emissions to be transported from La Merced by the north wind which prevails in this area, instead of due to differences in traffic patterns. The lack of considerable increases in black carbon and PPAH concentrations during other times of the day seems to indicate that there are no significant local sources of these emissions. PPAHs also appears to correlate with black carbon fairly well, except that sometimes PPAH concentration decreases earlier than black carbon (e.g. 4/17/2003 9:00 a.m. - 12 p.m. in Fig 3a), or it does not increase as significantly as black carbon (e.g. 4/20/2003 6:00 a.m. - 12 p.m. in Fig 3b). Such behavior is possible though, because as other materials coat the particles as they are processed and transported in the atmosphere, the PPAHs that are originally on the surface of the fresh particles can no longer be detected by the photoelectric aerosol sensor, which only measures surface PPAHs. Meanwhile, black carbon's optical absorption, and thus its detection by the aethalometer, would remain the same despite the hypothesized coating of the particles.

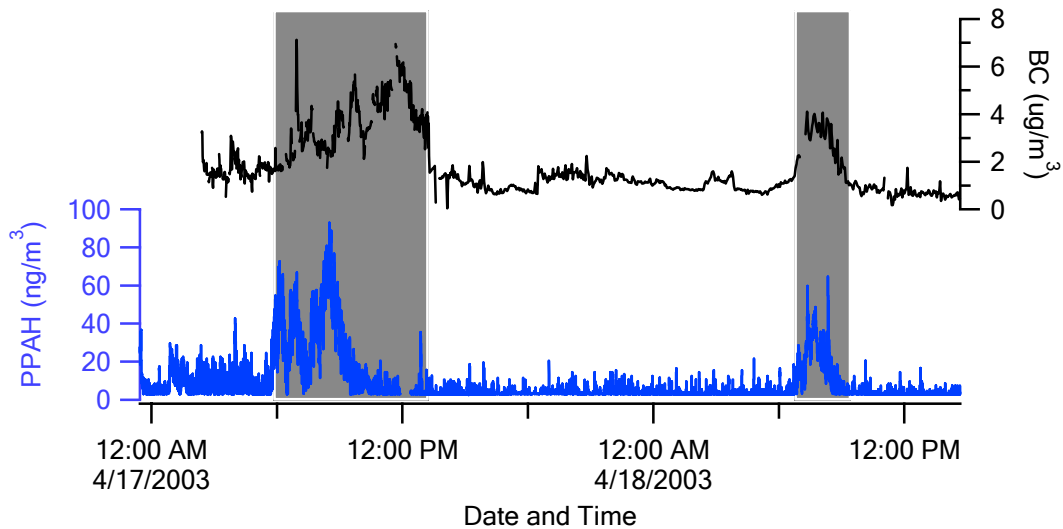


**Figure B.3a** Black carbon (BC) and PPAH concentrations measured at CENICA during the MCMA-2003 field campaign (April 17 – 18).

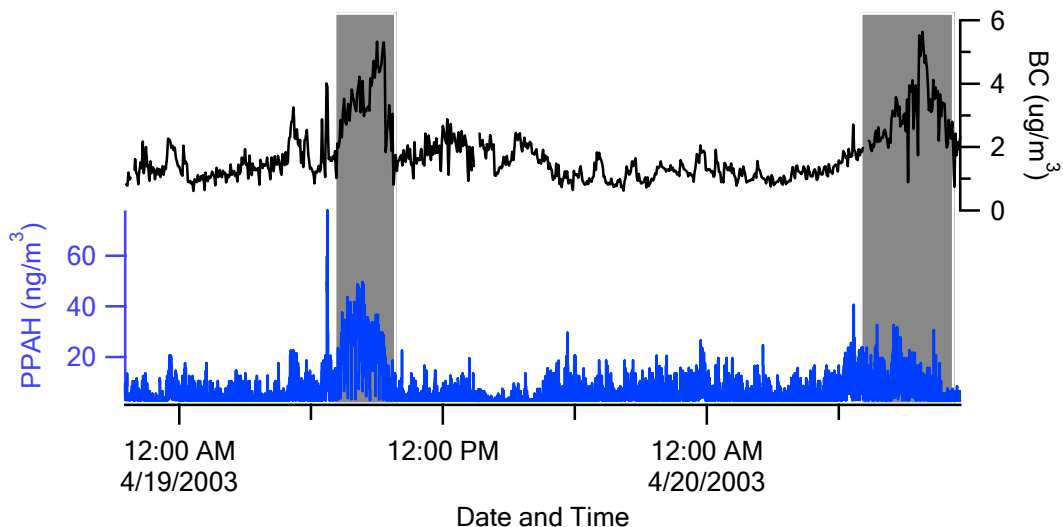


**Figure B.3b** Black carbon (BC) and PPAH concentrations measured at CENICA during the MCMA-2003 field campaign (April 19 – 20).

Farther to the southwest, we observe slightly higher black carbon concentrations at Pedregal than at CENICA. Even though Pedregal does not seem to have very important local sources of particles and is farther away from La Merced than CENICA is, Pedregal is directly downwind of La Merced, and it is closely confined by mountains to the southwest, which prevent the pollutants from being transported away and diluted. The peak period of black carbon and PPAH concentrations starts almost at the same time as at CENICA (Fig. 4). Generally, the diurnal pattern here is synchronized with what is found at La Merced, only with a one- hour time lag. This pattern suggests that the pollution in this area is directly influenced by sources in the city center. The same situation observed at CENICA—PPAH concentrations decreasing earlier than black carbon concentrations during the late morning hours—is also observed here.

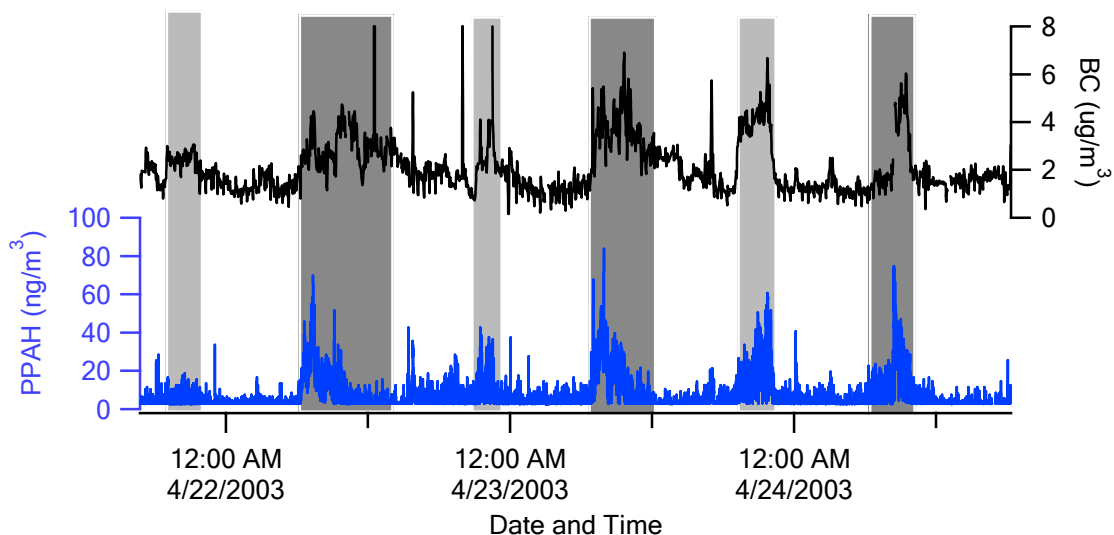


**Figure B.4** Black carbon (BC) and PPAH concentrations measured at Pedregal during the MCMA-2003 field campaign (April 22-23).

The lowest black carbon and PPAH concentrations among the four monitoring sites are measured at Santa Ana. The daily peak period of black carbon in this area does not start until after 11 a.m., about five hours later than in La Merced, and it can persist as late as 12 a.m. the next day (Fig. 5). Compared to other sites, PPAHs do not correlate as well with black carbon here. For example, there are regular increases in PPAHs in the morning, when no increase is observed for black carbon, indicating that there might be different types of particle sources in Santa Ana. The nighttime black carbon level is higher than the 24-hour average, which is not normal compared to the other sites. This could be caused by the day-long accumulation of the imported pollutants due to the poor ventilation capacity of this area, and the boundary layer shrinking in the evening. Alternatively, the presence of nighttime garbage burning near this site might also have contributed to elevated black carbon concentrations. Additional monitoring will be needed to confirm this pattern.

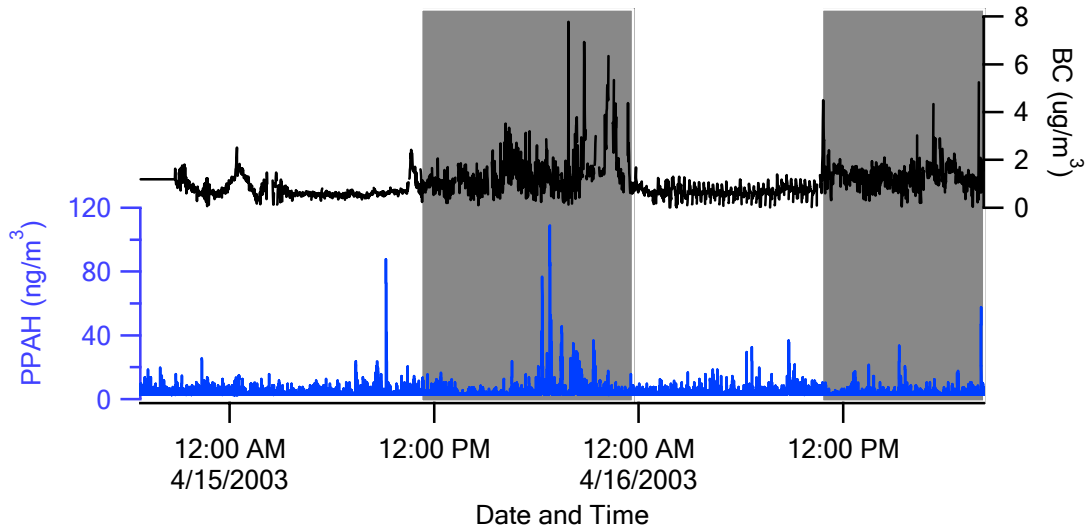


**Figure B.5** Black carbon (BC) and PPAH concentrations measured at Santa Ana during the MCMA-2003 field campaign (April 15-16).

### Conclusion

Concentrations of black carbon and PPAHS were measured at four locations in Mexico City. The spatial distribution and diurnal patterns of black carbon and PPAHS are presented. The highest concentrations are found at La Merced in the downtown area. Emissions in this area appear to contribute to the pollutant levels in other locations downwind, such as CENICA, Pedregal and Santa Ana. While motor vehicles are believed to be a major contributor to the pollutant emissions, the city's topographic and meteorological characteristics play an important role in exacerbating the air pollution problem in the MCMA.

## Appendix C

### Quality assurance of black carbon measurements

#### Black carbon measurements

During the MCMA-2003 field campaign, real-time black carbon concentrations were measured by an AE-16 Aethalometer (Magee Scientific Co, Berkeley, CA) running at a volume flow rate of 1-2 L min<sup>-1</sup>, depending on whether or not another instrument using the same inlet was also operating. The air sample first passed through a PM<sub>2.5</sub> cyclone to remove coarse particles. Because of its combustion origins, nearly all black carbon is expected to be found in particles smaller than 2.5 μm (Hansen 2003), so the size-selective inlet is not expected to affect the measurements. Measurements were recorded at one-, three- or five-minute intervals, depending on the operator's judgment in balancing time resolution against sensitivity, and saved to disk using the aethalometer's own floppy disk drive. Moreover, for quality control purpose, filtered air, also referred to as "zero-air" in this work, was injected into the system at regular intervals to calibrate the instruments.

#### Quality assurance procedure

The raw black carbon data have varying time resolutions and contain regularly occurring blank measurements and illogical negative values. Therefore, the data must go through extensive quality assurance and quality control (QA/QC) before being analyzed further.

##### 1. Correcting for calibration blanks

Zero-air is injected approximately once every 15 minutes for 20 seconds each time, which is shorter than the duration between consecutive aethalometer readings. So when the aethalometer reports concentrations at one-, three-, or five-minute intervals, the zero-air injection will affect the final readings, and this can happen as often as once every three data points (e.g. when the time resolution is selected to be 5 minutes). Indication of zero-air periods for the aethalometer is based on the ammonia (NH<sub>3</sub>) time series because the NH<sub>3</sub> instrument uses the same sampling inlet as aethalometer and has a reliable zero-air-marker time series associated with it. Rather than invalidating measurements affected by zero-air, we instead correct them using the equation below:

$$C_{BC,rev} = C_{BC,orig} \frac{t_o}{t_o - 20 \text{ s}} \quad (1)$$

$C_{BC,rev}$  - corrected value

$C_{BC,orig}$  - original value

$t_o$  - time duration between two readings (e.g., 60 s, 180 s or 300 s)

For black carbon data originally recorded at one-minute intervals in the fixed-site experiments, this correction factor gives unreasonable results, so we set all such points to NaN (not a number).

## 2. Correcting to the local pressure and converting units

The built-in algorithm of the aethalometer assumes an atmospheric pressure of 1 atm with its mass flow controller to calculate the black carbon concentration, and it expresses the concentration in  $\text{ng m}^{-3}$ . To correct the values to the local pressure in the MCMA, which is actually 0.75 atm, and to convert the units into  $\mu\text{g m}^{-3}$ , the original data are multiplied by 0.75 and 0.001.

## 3. Correcting the negative values

The algorithm that the aethalometer applies to calculate the black carbon concentration sometimes produces pairs of a large negative value followed by a large positive value, but the averages of these pairs fit in the expected concentration range quite well. Discussions with the aethalometer's developer and programmer confirmed that if the two values are averaged, the correct value is obtained (Hansen 2003, personal communication). So we average every negative value with the following positive value, set the result, if positive, to the second point and set NaN to the original negative point. This assignment, rather than setting both points to the average, is made because it is not realistic that two consecutive values are identical, and the negative data point, typically triggered by a "zero-air" period, is most likely be the problematic one. Otherwise, if the average remains negative, both points are set to NaN.

## 4. Rescaling the time series for uniform time resolution

In this step, the unevenly spaced data points are interpolated into a uniform time series with one-minute spacing, and the new series is named “k4\_bc\_aeth.” A new data mask “k4\_bc\_aeth\_dataMask” has also been created. The naming follows conventions specified in the data analysis plan developed by the MCMA-2003 campaign coordinators (Herndon 2003). The plan specifies formats and QA/QC procedures for all data collected by the mobile lab.

#### 5. Designating NARSTO flags

The data analysis plan also defines the flagging techniques that will allow perfectly consistent transfer to the NARSTO file format. The flagging rules used in generating the NARSTO flag series “k4\_bc\_aeth\_NARSTO\_tw” of black carbon data are presented in the table below.

**Table C.1** Data flags used for the QA-ed black carbon data.

<b>Data status</b>	<b>Flag</b>	<b>Meaning</b>
Originally valid	V0	valid value
Reevaluated due to zero air	V2	valid estimated value
Corrected due to pairing negative/positive data	V6	valid value but qualified due to non-standard sampling conditions
Originally assigned NaN	M1	missing value because no value is available
Assigned to NaN during QA/QC	M2	missing value because invalidated by data originator

#### References

Hansen, A. D. A. (2003). The Aethalometer, Magee Scientific Co.

Herndon, S., et al. (2003). Data Analysis Shedule MCMA 2003 (ARIMObAnalysis\_v3.doc).

## Appendix D

### IGOR Pro procedures

This section includes the IGOR procedures I wrote and used for QA, data analysis and emission factor calculations. QA\_BC is the master function to QA the black carbon data; DeltaConcact and a series of associated functions are intended to determine the natural variance range of CO<sub>2</sub> based on "parking measurements"; DataMaskMaker generates and saves data mask waves; and EmissionFactorCalc and the associated functions calculate the emission factors.

```
// Function name: QA_BC
// Takes experiment name, e.g. "F_20030404_CEN";
// Loads the waves, cuts the bc wave to the same time scale as the za file covers
// Averages the negative value of BC wave with its next point and get rid of the remaining negatives
// Reevaluates the bc values affected by za according to the NARSTO wave.
// Set 2 consecutive identical values in 1-min time series to NaN, mainly for "F" sites data.
// Rescale the unevenly-scaled BC waves to 1-min-intervaled ones.
// Also creates NARSTO_tw flags and _dataMask masks for BC as duplicates of the markers for za.
//Text wave POIS needs to be loaded before running the function.
```

Function **QA\_BC()**

```
string expt_name, za_dir, za_file, filedir_poi_bc
variable name_count, name_num
string save_waves, save_file
variable k0, k1, k2
variable tz1, tz2, tk0, tk1, tk2
variable p, x, nump
variable tf_1, tf_2
variable i, n, m, numt, k

loadwave/a/d/t "C:\\Documents and Settings\\meij.CE\\My Documents\\Research\\Data\\pois.itx"
wave /t pois = pois
name_num=numpts(pois)
for(name_count=0; name_count<name_num; name_count+=1)
    expt_name=pois[name_count]
```

```

// load Za file
za_dir = "C:\\Documents and Settings\\meij.CE\\My Documents\\Research\\POIs_za\\"
za_file = za_dir + expt_name + "_nh3_tdlc.itx"
loadwave/a/d/t za_file

// load data file aeth.itx and truncate the waves according to POI of za wave
loadwave/a/d/t "C:\\Documents and Settings\\meij.CE\\My Documents\\Research\\Data\\aeth.itx"
TrimWave2POI(d4_nh3_qcl, aethtime, aethbc)

//make new waves of bc based on the za wave of the same POI
Duplicate/o aethbc, k4_bc_aeth
Setscale/p x 0,1,"", aethbc
Setscale/p x 0,1,"", k4_bc_aeth
Duplicate/o aethtime, k4_bc_aeth_time
Setscale/p x 0,1,"dat", aethtime
Setscale/p x 0,1,"dat", k4_bc_aeth_time
m=numpnts(d4_nh3_qcl)-1
Make/n=(floor(m/60)) k4_bc_aeth_dataMask
SetScale/p x, k4_bc_aeth_time[0], 60, "dat", k4_bc_aeth_dataMask
k4_bc_aeth_dataMask[0,]=NaN
Make/t/n=(floor(m/60)) k4_bc_aeth_NARSTO_tw
SetScale/p x, k4_bc_aeth_time[0], 60, "dat", k4_bc_aeth_NARSTO_tw

//to convert the unit from ng/m3 into mg/m3 and to correct for Mexico City's reduced pressure
k4_bc_aeth*= 0.001*0.75

//average negative value with the next point
//remove any remaining negative value and convert the unit into mg/m3 from ng/m3
n=numpnts(k4_bc_aeth)
for(i=0; i<n; i+=1)
    if(k4_bc_aeth[i]<0)
        k4_bc_aeth[i]=(k4_bc_aeth[i]+k4_bc_aeth[i+1])/2
        k4_bc_aeth[i+1]=k4_bc_aeth[i]
        k4_bc_aeth_NARSTO_tw[x2pnt(k4_bc_aeth_NARSTO_tw, k4_bc_aeth_time[i])]="V6"
        k4_bc_aeth_NARSTO_tw[x2pnt(k4_bc_aeth_NARSTO_tw, k4_bc_aeth_time[i+1])]="V6"
        k4_bc_aeth_dataMask[x2pnt(k4_bc_aeth_dataMask, k4_bc_aeth_time[i])]=1
        k4_bc_aeth_dataMask[x2pnt(k4_bc_aeth_dataMask, k4_bc_aeth_time[i+1])]=1
        if(k4_bc_aeth[i]<0)
            k4_bc_aeth[i]=NaN
            k4_bc_aeth[i+1]= NaN

```

```

        k4_bc_aeth_NARSTO_tw[x2pnt(k4_bc_aeth_NARSTO_tw, k4_bc_aeth_time[i])]="M2"
        k4_bc_aeth_NARSTO_tw[x2pnt(k4_bc_aeth_NARSTO_tw, k4_bc_aeth_time[i+1])]="M2"
        k4_bc_aeth_dataMask[x2pnt(k4_bc_aeth_dataMask, k4_bc_aeth_time[i])]=0
        k4_bc_aeth_dataMask[x2pnt(k4_bc_aeth_dataMask, k4_bc_aeth_time[i+1])]=0
    endif
endif
endfor

//reevaluate ZA-affected values
n=numpnts(d4_nh3_qcl_NARSTO_tw)
for(i=0; i<n; i+=1)
    if(DetectZAFlag(d4_nh3_qcl_NARSTO_tw, i) == 1)
        //the for loop below is to count the "number of successive ZA flags (p)" following k4_bc_aeth_NARST_tw[i]
        for(p=0; p<=n; p+=1) // f is a flag that will indicate where ZA period stops
            //the for loop below is to check whether there's ZA flag in k4_bc_aeth_NARST_tw[i+1]
            if(DetectZAFlag(d4_nh3_qcl_NARSTO_tw, i) ==0)
                break
            else
                i+=1
            endif
        endfor
    endif

    //find the point number "k" in k4_bc_aeth of the nearest corresponding time, the "i-th" point in nh3 wave (or the
    k4_bc_aeth_narsto wave)& make sure that ZA period occurs before k
    tz1=pnt2x(d4_nh3_qcl_NARSTO_tw, i-p)
    tz2=pnt2x(d4_nh3_qcl_NARSTO_tw, i)
    nump=numpnts(k4_bc_aeth_time)
    for(x=0; x<nump; x+=1)
        if(k4_bc_aeth_time[x]>=tz2)
            tk2= k4_bc_aeth_time[x]
            tk1= k4_bc_aeth_time[x-1]
            tk0= k4_bc_aeth_time[x-2]
            tf_1= k4_bc_aeth_time[x]>=3132409560.000 && k4_bc_aeth_time[x]<=3132894480.000
            tf_2 = k4_bc_aeth_time[x]>=3133188780.000 && k4_bc_aeth_time[x]<=3133430220.000
            //2 possibilities of the relation between where the ZA period falls and the position of k2, k1, k0.
            if( tk1 <= tz1)//If the ZA period is between point x-1 and x
                if((tf_1 || tf_2) &&!cmpstr(expt_name[0],"F"))//If it's 1-min spaced fixed-site experiment
                    k4_bc_aeth[x]=NaN
                    k4_bc_aeth_NARSTO_tw[x2pnt(k4_bc_aeth_NARSTO_tw, k4_bc_aeth_time[x])]="M2"
                endif
            endif
        endif
    endfor
endfor

```

```

        k4_bc_aeth_dataMask[x2pnt(k4_bc_aeth_dataMask, k4_bc_aeth_time[x])]=0
        break
    else
        k4_bc_aeth[x]*= (tk2 - tk1)/((tk2 - tk1) - (tz2- tz1))
        k4_bc_aeth_NARSTO_tw[x2pnt(k4_bc_aeth_NARSTO_tw, k4_bc_aeth_time[x])]="V2"
        k4_bc_aeth_dataMask[x2pnt(k4_bc_aeth_dataMask, k4_bc_aeth_time[x])]=1
    endif
else//If the ZA period is between point x-2 and x-1
    if((tf_1 || tf_2)&&(!cmpstr(expt_name[0],"F")))
        k4_bc_aeth[x]=NaN
        k4_bc_aeth[x-1]=NaN
        k4_bc_aeth_NARSTO_tw[x2pnt(k4_bc_aeth_NARSTO_tw, k4_bc_aeth_time[x])]="M2"
        k4_bc_aeth_NARSTO_tw[x2pnt(k4_bc_aeth_NARSTO_tw, k4_bc_aeth_time[x-1])]="M2"
        k4_bc_aeth_dataMask[x2pnt(k4_bc_aeth_dataMask, k4_bc_aeth_time[x])]=0
        k4_bc_aeth_dataMask[x2pnt(k4_bc_aeth_dataMask, k4_bc_aeth_time[x-1])]=0
        break
    else
        k4_bc_aeth[x]*= (tk2 - tk1)/(tk2 - tz2)
        k4_bc_aeth[x-1]*= (tk1 - tk0)/(tz1- tk0)
        k4_bc_aeth_NARSTO_tw[x2pnt(k4_bc_aeth_NARSTO_tw, k4_bc_aeth_time[x])]="V2"
        k4_bc_aeth_NARSTO_tw[x2pnt(k4_bc_aeth_NARSTO_tw, k4_bc_aeth_time[x-1])]="V2"
        k4_bc_aeth_dataMask[x2pnt(k4_bc_aeth_dataMask, k4_bc_aeth_time[x])]=1
        k4_bc_aeth_dataMask[x2pnt(k4_bc_aeth_dataMask, k4_bc_aeth_time[x-1])]=1
    endif
endif
break
endif
endif
endif
endfor

//rescale bc wave to 1 min time scale by interpolation
Make/n=(floor(m/60)) k4_bc_aeth_1min
setscale/p x, k4_bc_aeth_time[0], 60, "dat", k4_bc_aeth_1min
n=numpnts(k4_bc_aeth_1min)
for(i=0,k=0;i<n;i+=1)
    tf_1= k4_bc_aeth_time[i]>=3132409560.000 && k4_bc_aeth_time[i]<=3132894480.000
    tf_2 = k4_bc_aeth_time[i]>=3133188780.000 && k4_bc_aeth_time[i]<=3133430220.000
    if (!(tf_1||tf_2))

```

```

        k4_bc_aeth_1min[i]=interp(pnt2x(k4_bc_aeth_1min,i), k4_bc_aeth_time, k4_bc_aeth)
    else
        k4_bc_aeth_1min[i]=k4_bc_aeth[i-k]
        if((k4_bc_aeth_time[i-k+1]-k4_bc_aeth_time[i-k])>60)
            numt=(k4_bc_aeth_time[i-k+1]-k4_bc_aeth_time[i-k])/60-1
            k4_bc_aeth_1min[i+1,i+numt]=NaN
            i+=numt
            k+=numt
        endif
    endif
endfor
killwaves k4_bc_aeth
rename k4_bc_aeth_1min k4_bc_aeth

// Make new NARSTO & dataMask waves on 1 min time spacing
n=numpts(k4_bc_aeth)
for(i=0; i<n; i+=1)
    if(numtype(k4_bc_aeth[i])==2 && numtype(k4_bc_aeth_dataMask[i])==2)
        k4_bc_aeth_NARSTO_tw[i]="M1"
        k4_bc_aeth_dataMask[i]= 0
    elseif(numtype(k4_bc_aeth[i])!=2 && numtype(k4_bc_aeth_dataMask[i])==2)
        k4_bc_aeth_NARSTO_tw[i]="V0"
        k4_bc_aeth_dataMask[i]=1
    endif
endfor

//save itx file
filedir_poi_bc ="C:\\Documents and Settings\\meij.CE\\My Documents\\Research\\POIs\\"+expt_name+"\\"
save_file = filedir_poi_bc + expt_name + "_bc_aeth.itx"
save_waves ="k4_bc_aeth;k4_bc_aeth_NARSTO_tw;k4_bc_aeth_dataMask;"
Save/O/T/M="\r\n"/B save_waves as save_file

//kill all waves
killwaves/Z d4_nh3_qcl, d4_nh3_qcl_NARSTO_tw, d4_nh3_qcl_dataMask, d4_nh3_qcl_use
killwaves/Z k4_bc_aeth, k4_bc_aeth_time, k4_bc_aeth_NARSTO_tw, k4_bc_aeth_dataMask
killwaves/Z aethtime, aethbc
endfor
end

```

```

function TrimWave2POI(poi_wave, wave1, wave2)
    Wave poi_wave, wave1, wave2

    Variable pt_start=2, pt_end
    variable x_start, x_end
    variable i, n
    x_start= pnt2x(poi_wave, 0)
    x_end=pnt2x(poi_wave, numpts(poi_wave)-1)
    n=numpts(wave1)
    for(i=0;i<n;i+=1)
        if (x_start>=wave1[i])
            pt_start= i+1
        elseif(x_end<=wave1[i])
            pt_end= i
            break
        endif
    endfor

    duplicate/o/r=(pt_start, pt_end) wave1, new_w1
    duplicate/o/r=(pt_start, pt_end) wave2, new_w2
    killwaves wave1, wave2
    rename new_w1, aethtime
    rename new_w2, aethbc
end

```

```

Function DetectZaFlag(wave_tw, i)
    Wave/t wave_tw
    Variable i

    Variable j, m
    m=ItemsInList (wave_tw[i])
    for(j=0; j<m; j+=1 )
        if(!cmpstr(StringFromList(j, wave_tw[i]), "ZA"))
            return 1
        elseif(j+1==m)
            return 0
        endif
    endfor
end

```

```

//Function name: DELTACONCAT
//"Delta" - CO2 concentration increase above the baseline
//"Concat" - concatenating all the delta values from the parking time period
//Text wave PARKINGTIME_LIST needs to be loaded prior to running the function
//PARKINGTIME_LIST contains the names of POIs that have parking data and the starting and ending point number of the parking
time period.
//When the function completes, 95 percentile of the sorted DELTA_CONCATENATED wave is set to be the theshold of background
measurements.

```

Function **DeltaConcat()**

```

Killwaves/Z delta_concatenated
Wave/T parkingtime_list=parkingtime_list
String parkingtime, POI
String/G species_name
String mainfolder="C:\\Documents and Settings\\meij.CE\\My Documents\\Research\\"
Variable startP, endP
Variable j,m=numpts(parkingtime_list),i,n
For(j=0;j<m;j+=1)
    parkingtime=parkingtime_list[j]
    POI=StringFromList(0,parkingtime)
    startP=str2num(StringFromList(1,parkingtime))
    endP=str2num(StringFromList(2,parkingtime))

    Loadwave/a/d/o/t mainfolder+"POIs\\"+POI+"\\"+POI+"_methanol_ptr.itx"
    Killwaves/Z d4_methanol_ptr_orig, d4_methanol_dataMask_orig
    Rename d4_methanol_ptr, d4_methanol_ptr_orig
    Rename d4_methanol_ptr_dataMask, d4_methanol_dataMask_orig
    Duplicate/d/o/R=[startP,endP] d4_methanol_ptr_orig, d4_methanol_ptr
    Duplicate/d/o/R=[startP,endP] d4_methanol_dataMask_orig, d4_methanol_ptr_dataMask

    Loadwave/a/d/o/t mainfolder+"POIs\\wind\\"+POI+"_sonic.itx"
    Killwaves/Z d4_WindTruck_Degree_orig
    Rename d4_WindTruck_Degree, d4_WindTruck_Degree_orig
    Duplicate/d/o/R=[startP,endP] d4_WindTruck_Degree_orig, d4_WindTruck_Degree

    species_name="methanol"
    PeakPicker_Self()
    Wave PeakMarker_self=PeakMarker_self

```

```

Loadwave/a/d/o/t mainfolder+"POIs\\"+POI+"\\"+POI+"_licor1.itx"
Killwaves/Z d4_co2_licor1_orig, d4_co2_dataMask_orig
Rename d4_co2_licor1, d4_co2_licor1_orig
Rename d4_co2_licor1_dataMask, d4_co2_dataMask_orig
Duplicate/d/o/R=[startP,endP] d4_co2_licor1_orig, d4_co2_licor1, delta
Duplicate/d/o/R=[startP,endP] d4_co2_dataMask_orig, d4_co2_licor1_dataMask
DataMask(d4_co2_licor1)
species_name="co2"
Background(d4_co2_licor1)
Wave bkgd_co2=bkgd_co2
delta=d4_co2_licor1-bkgd_co2
n=numpts(delta)
For(i=0;i<n;i+=1)
    If(PeakMarker_self[i]!=0||d4_co2_licor1[i]>600||delta[i]<0)
        //If CO2 is higher than 600 ppm, then it is suspected that it's from some nearby point sources
        delta[i]=NaN
    Endif
Endfor
Print "POI:", POI
wavestats delta
ConcatenateWaves("delta_concatenated","delta")
Endfor
Print "*****Concatenated delta wave*****"
wavestats delta_concatenated
duplicate/o delta_concatenated, delta_con_sort
sort delta_con_sort, delta_con_sort
Edit delta_con_sort.id

```

End

// Function PEAKMARKERWAVES generates and saves peak marker waves in to designated folders.

// Text wave POIS needs to be loaded before running the function

// POIS contains the names of those mobile POIs that have all the necessary data, such as ptr waves to generate peak marker waves.

Function **PeakMarkerWaves**(criterion)

Variable criterion//the threshold value of background measurements, eg: 42 ppm

Wave/t pois=pois

String/G POI, species\_name

String/G mainfolder="C:\\Documents and Settings\\meij.CE\\My Documents\\Research\\"

```

String save_file=mainfolder+"POIs\\"+POI+"\\"+POI+"_ratios.itx"
Variable poi_num, poi_count
poi_num=numpts(pois)
For(poi_count=0; poi_count<poi_num; poi_count+=1)
    POI=pois[poi_count]
    //Load co2, methanol and wind direction waves
    Loadwave/a/d/o/t mainfolder+"POIs\\"+POI+"\\"+POI+"_licor1.itx"
    Loadwave/a/d/o/t mainfolder+"POIs\\"+POI+"\\"+POI+"_methanol_ptr.itx"
    Loadwave/a/d/o/t mainfolder+"POIs\\"+POI+"\\"+POI+"_velo.itx"
    Loadwave/a/d/o/t mainfolder+"POIs\\wind\\"+POI+"_sonic.itx"
    DataMask(d4_co2_licor1)
    species_name="co2"
    Background(d4_co2_licor1)
    species_name="methanol"
    PeakPicker_Self()
    CO2marker(criterion)
Endfor
End

```

#### Function **PeakPicker\_Self()**

```

//This function generates waves that mark out the time points...
//... when certain pollutant species exceeds its particular threshold values, or concentration "peak height".

```

```

Wave d4_methanol_ptr=d4_methanol_ptr
Wave d4_WindTruck_Degree=d4_WindTruck_Degree
SVAR species_name

DataMask(d4_methanol_ptr)
Background(d4_methanol_ptr)
Wave bkgd="$bkgd_"+species_name

Duplicate/d/o d4_methanol_ptr, PeakMarker_self
Variable i, n=numpts(d4_methanol_ptr), peakheight
For(i=0;i<n;i+=1)
    peakheight=bkgd[i]+30//Eliminate points above "BaseValue+30"
    If(numtype(d4_methanol_ptr[i])!=0)
        PeakMarker_self[i]=NaN
    elseif(d4_methanol_ptr[i]-bkgd[i]>=peakheight)
        PeakMarker_self[i]=1
    end
End

```

```

                elseif((d4_WindTruck_Degree[i]>=90)&&(d4_WindTruck_Degree[i]<=300))
                    PeakMarker_self[i]=1
                else
                    PeakMarker_self[i]=0
                endif
            Endfor
        End

```

Function **CO2marker**(criterion)

Variable criterion

SVAR mainfolder=mainfolder

SVAR POI=POI

Wave d4\_co2\_licor1=d4\_co2\_licor1

Wave bkgd\_co2=bkgd\_co2

Wave PeakMarker\_self=PeakMarker\_self

Variable i,n=numpts(d4\_co2\_licor1)

Duplicate/O d4\_co2\_licor1, wave\_peakmarker

For(i=0;i<n;i+=1)

    If (numtype(d4\_co2\_licor1[i])==2)

        wave\_peakmarker[i]=Nan//invalid data

    elseif(PeakMarker\_self[i]==1)

        wave\_peakmarker[i]=-1//self-sampling

    elseif(numtype(PeakMarker\_self[i])==2)

        wave\_peakmarker[i]=Nan

    elseif((d4\_co2\_licor1[i]-bkgd\_co2[i])>criterion)

        wave\_peakmarker[i]=1//exhaust plume

    else

        wave\_peakmarker[i]=0//background

    endif

endfor

String save\_file=mainfolder+"POIs\\"+POI+"\\"+POI+"\_peakmarker.itx"

Save/O/B/T "wave\_peakmarker" as save\_file

End

//Function DATAMASKMAKER generates data mask waves for specified species...

//... and save the data waves, NARSTO text waves and dataMask waves as one igor text file in the respective POI folders.

```
//The function sets those "V0", "V2", "V3" and "V7" flags who are not coupled with "ZA" or "ZP" to mask value 1;
//and all the other flags to mask value 0.
//Text wave POIS_EFC needs to be loaded prior to running the function.
```

Function **dataMaskmaker**(species, instrument, itxSuffix)

String species, instrument, itxSuffix

Wave/t pois=pois\_EFC

String POI, flagList

String workwavename="d4\_"+species+"\_"+instrument

String workwaveNARSTOname="d4\_"+species+"\_"+instrument+"\_narsto\_tw"

String workwaveDataMaskname="d4\_"+species+"\_"+instrument+"\_dataMask"

If(cmpstr("bc", species)==0)

workwavename="k4\_"+species+"\_"+instrument

workwaveNARSTOname="k4\_"+species+"\_"+instrument+"\_narsto\_tw"

workwaveDataMaskname="k4\_"+species+"\_"+instrument+"\_dataMask"

Endif

Variable POIindex, POIcount=numpts(pois), index, icount, fdex

For(POIindex=0;POIindex<POIcount;POIindex+=1)

POI=pois[POIindex]

Loadwave/a/d/o/t "C:\\Documents and Settings\\meij.CE\\My Documents\\Research\\POIs\\"+POI+"\\"+POI+"\_"+itxSuffix+".itx"

Wave workwave=\$workwavename

Wave/t workwaveNARSTO=\$workwaveNARSTOname

Duplicate/o/d workwave, workwaveDataMask

workwaveDataMask=Nan

icount=numpts(workwave)

For(index=0;index<icount;index+=1)

flagList=workwaveNARSTO[index]

If(ItemsInList(flagList)==1)

If(cmpstr("V0", StringFromList(0,flagList))==0||cmpstr("V2", StringFromList(0,flagList))==0||cmpstr("V3",

StringFromList(0,flagList))==0||cmpstr("V7", StringFromList(0,flagList))==0)

workwaveDataMask[index]=1

Endif

else

For(fdex=0;fdex<ItemsInList(flagList);fdex+=1)

If(cmpstr("ZA", StringFromList(fdex,flagList))==0||cmpstr("ZP", StringFromList(fdex,flagList))==0)

workwaveDataMask[index]=NaN

break

```

                Endif
                If(cmpstr("V0", StringFromList(fdex,flagList))==0)
                    workwaveDataMask[idex]=1
                Endif
            Endfor
        Endif
    Endfor
    Killwaves/z $workwaveDataMaskname
    Duplicate/o/d workwaveDataMask, $workwaveDataMaskname
    String save_wave, save_file="C:\\Documents and Settings\\meij.CE\\My
Documents\\Research\\POIs\\"+POI+"\\"+POI+"_"+"species+"_"+"instrument+" ".itx"
    StrSwitch (species)
        Case "co":
            save_wave="d4_co_wsu;d4_co_wsu_narsto_tw;d4_co_wsu_dataMask"
            break
        Case "benzene":
            save_wave="d4_benzene_ptr;d4_benzene_ptr_narsto_tw;d4_benzene_ptr_dataMask"
            break
        Case "noy":
            save_wave="d4_noy_mit;d4_no_mit;d4_noy_mit_narsto_tw;d4_no_mit_narsto_tw;d4_noy_mit_dataMask"
            break
        Case "bc":
            save_wave="k4_bc_aeth;k4_bc_aeth_narsto_tw;k4_bc_aeth_dataMask"
            break
        Case "pah":
            save_wave="d4_pah_pas;d4_pah_pas_narsto_tw;d4_pah_pas_dataMask"
        Case "methanol":
            save_wave="d4_methanol_ptr;d4_methanol_ptr_narsto_tw;d4_methanol_ptr_dataMask"
    EndSwitch
    Save/O/T/M="\r\n"/B save_wave as save_file
Endfor
End

```

//Function name: EmissionFactorCalc

//This function is to calculate the emission factors of BC, PPAHs, CO, benzene, VOCs and NOy.

//Text waves "POIS\_EFC" and WORKWAVELIST need to be loaded prior of running the function.

//POIS\_EFC contains the names of 13 mobile POIs that are considered in calculating the emission factors;

//WORKWAVELIST contains the data wave names of the five species.

//When the function completes, wave statistics of the concatenated emission factor waves are printed in the command window.

Function **EmissionFactorCalc()**

```
Killwaves/Z EF_concatenated_pah, EF_concatenated_bc, EF_concatenated_co, EF_concatenated_benzene, EF_concatenated_noy
Wave/t pois=pois_EFC
Wave/t workwavelist=workwavelist
String/G POI, species_name, instruname
String/G workwavename//workwavename: eg. "d4_bc_aeth"
```

```
Variable poi_dex, poi_count, species_dex
```

```
poi_count=numpts(pois)
```

```
For(poi_dex=0; poi_dex<poi_count; poi_dex+=1)
```

```
    POI=pois[poi_dex]
```

```
    String/G mainpath="C:\\Documents and Settings\\meij.CE\\My Documents\\Research\\POIs\\"+POI+"\\ "+POI+"_"
```

```
    Loadwave/a/d/o/t mainpath+"licor1.itx"//Loading CO2 and wave_peakmarker waves
```

```
    DataMask(d4_co2_licor1)
```

```
    species_name="co2"
```

```
    Background(d4_co2_licor1)
```

```
    Loadwave/a/d/o/t mainpath+"peakmarker.itx"
```

```
For(species_dex=0;species_dex<5;species_dex+=1)
```

```
//Reading wave names for each species
```

```
    workwavename=workwavelist[species_dex]
```

```
    species_name=workwavename[3,strsearch(workwavename,"_",3)-1]
```

```
    instruname=workwavename[strsearch(workwavename,"_",3)+1, strlen(workwavename)-1]
```

```
    Loadwave/a/d/o/t mainpath+species_name+"_"+instruname+".itx"//Loading data waves for each species
```

```
    Wave workwave=$workwavename
```

```
//Processing individual species and calculationg P/CO2 ratios
```

```
StrSwitch (species_name)
```

```
    Case "co" :
```

```
        DataMask(workwave)
```

```
        Background(workwave)
```

```
        RatioCalc_multisec(workwave,10)
```

```
        Wave ratiowave=ratiowave
```

```
        Duplicate/d/o ratiowave, ratio_co_co2
```

```
        Wave eventmarker=eventmarker
```

```
        Duplicate/d/o eventmarker, eventmarker_co
```

```
        Break
```

```

Case "benzene":
  Loadwave/a/d/o/t mainpath+"PTR.itx"
  //Loading data waves for each species
  Wave d4_benzene_ptr=d4_benzene_ptr
  Wave d4_c2benzene_ptr=d4_c2benzene_ptr
  Wave d4_c3benzene_ptr=d4_c3benzene_ptr
  d4_benzene_ptr=d4_benzene_ptr-0.092*(d4_c2benzene_ptr-d4_benzene_ptr)-0.065*(d4_c3benzene_ptr-
d4_benzene_ptr)
  DataMask(workwave)
  Background(workwave)
  RatioCalc_1sec(workwave)
  Duplicate/d/o ratiowave, ratio_benzene_co2
  Break
Case "bc":
  DataMask(k4_bc_aeth)
  Rescale_BC()
  Background(workwave)
  RatioCalc_1sec(workwave)
  Duplicate/d/o ratiowave, ratio_bc_co2
  Break
Case "pah":
  DataMask(workwave)
  Rescale_PAH()
  Wave d4_pah_pas_rs=d4_pah_pas_rs
  workwavename="d4_pah_pas_rs_interp"
  Background(workwave)
  RatioCalc_multisec(workwave,30)
  Duplicate/d/o ratiowave, ratio_pah_co2
  Wave eventmarker=eventmarker
  Duplicate/d/o eventmarker, eventmarker_pah
  Break
Case "noy":
  DataMask(workwave)
  Background(workwave)
  RatioCalc_multisec(workwave,10)
  Wave eventmarker=eventmarker
  Duplicate/d/o eventmarker, eventmarker_noy
  Duplicate/d/o ratiowave, ratio_noy_co2
EndSwitch

```

Endfor

```

//Calculating the emission factor for individual points (g P/kg fuel)
Variable i,j,n=numpts(d4_co2_licor1)
Variable ratio_co_avg, ratio_benzene_avg, ratio_voc_avg,A=2.3E6
//A in ppm CO2/kg fuel
Duplicate/d/o d4_co2_licor1, EF_pah, EF_bc, EF_co, EF_benzene, EF_noy, EF_VOC
EF_pah=NaN; EF_bc=NaN; EF_co=NaN; EF_benzene=NaN; EF_noy=NaN; EF_VOC=NaN
Duplicate/d/o ratio_benzene_co2, ratio_voc_co2
For(i=0;i<n;i+=1)
  If(eventmarker_pah[i]==1)//pah
    Wavestats/Q/R=[i-29,i] ratio_co_co2
    ratio_co_avg=V_avg
    Wavestats/Q/R=[i-29,i] ratio_benzene_co2
    ratio_benzene_avg=V_avg
    ratio_voc_avg=ratio_benzene_avg*0.001*97.5*3.12
    EF_pah[i]=(ratio_pah_co2[i])*1E-9/(1+ratio_co_avg+ratio_voc_avg)*A
  Endif
  If(eventmarker_co[i]==1)//co, benzene, voc, bc, noy
    Wavestats/Q/R=[i-9,i] ratio_benzene_co2
    ratio_benzene_avg=V_avg
    ratio_voc_avg=ratio_benzene_avg*0.001*97.5*3.12
    EF_co[i]=(ratio_co_co2[i])*3.07E-5*28/(1+ratio_co_co2[i]+ratio_voc_avg)*A
    EF_benzene[i]=ratio_benzene_avg*1E-3*3.07E-5*78/(1+ratio_co_co2[i]+ratio_voc_avg)*A
    EF_VOC[i]=ratio_voc_avg*1E-3*3.07E-5*12/(1+ratio_co_co2[i]+ratio_voc_avg)*A
    Wavestats/Q/R=[i-9,i] ratio_bc_co2
    EF_bc[i]=V_avg*1E-6/(1+ratio_co_co2[i]+ratio_voc_avg)*A
    EF_noy[i]=(ratio_noy_co2[i])*1E-3*3.07E-5*46/(1+ratio_co_avg+ratio_voc_avg)*A
  Endif
Endfor
RatioConCat(EF_pah)
RatioConCat(EF_bc)
RatioConCat(EF_co)
RatioConCat(EF_benzene)
RatioConCat(EF_noy)
RatioConCat(EF_VOC)

Endfor

Wave EF_concatenated_pah=EF_concatenated_pah

```

```
Print "EF_concatenated_pah"  
WaveStats EF_concatenated_pah  
Make/o/d/n=500, histowave_pah  
Histogram/b={0,0.002,500} EF_concatenated_pah, histowave_pah
```

```
Wave EF_concatenated_bc=EF_concatenated_bc  
Print "EF_concatenated_bc"  
WaveStats EF_concatenated_bc  
Make/o/d/n=500, histowave_bc  
Histogram/b={0,0.1,500} EF_concatenated_bc, histowave_bc
```

```
Wave EF_concatenated_co=EF_concatenated_co  
Print "EF_concatenated_co"  
WaveStats EF_concatenated_co  
Make/o/d/n=500, histowave_co  
Histogram/b={0,10,500} EF_concatenated_co, histowave_co
```

```
Wave EF_concatenated_benzene=EF_concatenated_benzene  
Print "EF_concatenated_benzene"  
WaveStats EF_concatenated_benzene  
Make/o/d/n=500, histowave_benzene  
Histogram/b={0,0.1,500} EF_concatenated_benzene, histowave_benzene  
Print "EFvoc=EFbenzene*53.6=", V_avg*53.6,"g voc/L fuel"
```

```
Wave EF_concatenated_VOC=EF_concatenated_VOC  
Print "EF_concatenated_VOC (g C/L fuel)"  
WaveStats EF_concatenated_VOC
```

```
Wave EF_concatenated_noy=EF_concatenated_noy  
Print "EF_concatenated_noy"  
WaveStats EF_concatenated_noy  
Make/o/d/n=500, histowave_noy  
Histogram/b={0,5,500} EF_concatenated_noy, histowave_noy
```

End

```
Function DataMask(workwave)//Removing points with "bad" flags  
Wave workwave  
Wave dataMaskwave=$Nameofwave(workwave)+"_dataMask"  
workwave*=dataMaskwave
```

End

Function **Background**(workwave)

Wave workwave

SVAR species\_name

String bkgdwavename="bkgd\_"+species\_name

Variable i,n=numpts(workwave)

Variable winWidth=60\*3//Window width selected to be 3 min

Variable mWin\_start, j, min\_idx

Make/d/o/n=(n) bkgd

SetScale/P x pnt2x (workwave, 0),1,"dat", bkgd

for(i=0; i<n; i+=winWidth)

    Duplicate/O/D/R=[i,i+winWidth-1] workwave, wave\_movwin

    WaveStats/Q wave\_movwin

    Sort wave\_movwin, wave\_movwin

    bkgd[i, i+winWidth-1]= wave\_movwin[5]//Assigning 5th lowest as the bkgd value for the entire window

endfor

SmoothBaseline(bkgd)

Killwaves/z \$"bkgd\_"+species\_name

Rename bkgd \$"bkgd\_"+species\_name

End

Function **SmoothBaseline**(workbkgd)

Wave workbkgd

Duplicate/o/d workbkgd, bkgd\_temp, bkgd\_NaNmarker, bkgd\_smoothed

bkgd\_temp=NaN;bkgd\_NaNmarker=Nan

SetScale/P x 0,1,"", bkgd\_temp

Variable i,n=numpts(bkgd),j

For(i=0,j=0;i<n;i+=1)

    If(numtype(workbkgd[i])!=2)

        bkgd\_temp[j]=workbkgd[i]

        j+=1

    Else

        bkgd\_NaNmarker[i]=1

    Endif

Endfor

Smooth 1000, bkgd\_temp

For(i=0,j=0;i<n;i+=1)

    If(bkgd\_nanmarker[i]==1)

```

                bkgd_smoothed[i]=NaN
            Else
                bkgd_smoothed[i]=bkgd_temp[j]
                j+=1
            Endif
        Endfor
    Duplicate/d/o bkgd_smoothed, bkgd
End

```

```

Function RatioCalc_1sec(polu_wave)
//Ratio calculations of work waves with 1 sec resolution, e.g. BC and benzene
    Wave polu_wave

```

```

    Wave wave_peakmarker=wave_peakmarker
    Wave d4_co2_licor1=d4_co2_licor1
    Wave bkgd_co2=bkgd_co2
    SVAR/Z species_name=species_name
    Wave bkgd_polu=$( "bkgd_" +species_name)
    Duplicate/O d4_co2_licor1, ratiowave
    ratiowave=NaN

```

```

    Duplicate/o polu_wave, delta_polu
    Duplicate/o d4_co2_licor1, delta_co2
    delta_polu=polu_wave-bkgd_polu
    delta_co2=d4_co2_licor1-bkgd_co2
    ratiowave=delta_polu/delta_co2
    Variable i,n=numpts(d4_co2_licor1)
    For(i=0;i<n;i+=1)
        If(ratiowave[i]<0||numtype(ratiowave[i])!=0||delta_co2[i]<1||delta_polu[i]<1||wave_peakmarker[i]!=1)
            ratiowave[i]=NaN //ratiowave only contains plume points
        endif
    Endfor

```

```

End

```

```

Function RatioCalc_multisec(polu_wave, time_resolution)
//Ratio calculations for PAH(TR=30s), co(TR=30s) and noy(TR=30s)
    Wave polu_wave
    Variable time_resolution

    SVAR/Z species_name=species_name

```

```

Wave d4_co2_licor1=d4_co2_licor1
Wave wave_peakmarker=wave_peakmarker
Wave bkgd_polu="$bkgd_"+species_name
Wave bkgd_co2=bkgd_co2
Duplicate/o polu_wave, delta_polu
Duplicate/o d4_co2_licor1, delta_co2, ratiowave, eventmarker
delta_polu=polu_wave-bkgd_polu
delta_co2=d4_co2_licor1-bkgd_co2
ratiowave=NaN;eventmarker=NaN
Variable i,j,n=numpts(polu_wave), plume_count,bkgd_count,self_count,co2_avg
For(i=0;i<n;i+=1)
    plume_count=0;bkgd_count=0;self_count=0;j=0
    Do
        Switch (wave_peakmarker[i+j])
            Case 1:
                plume_count+=1
                break
            Case 0:
                bkgd_count+=1
                break
            Case -1:
                self_count+=1
                break
        EndSwitch
        j+=1
    While(j<time_resolution)
    If(plume_count>=(time_resolution*0.8))//plume-measurements more than 80%
        WaveStats/Q/R=[i, i+time_resolution-1] delta_co2
        co2_avg=V_avg
        WaveStats/Q/R=[i, i+time_resolution-1] delta_polu
        ratiowave[i+time_resolution-1]=V_avg/co2_avg
        eventmarker[i+time_resolution-1]=1
        i+=time_resolution-2

//Following steps are skipped, so that ratiowave only contains plume points;
//they can be activated if generating ratios of background and self measurements are desired.
//Elseif(bkgd_count>=time_resolution*0.8)//background-measurements more than 80%
//    WaveStats/Q/R=[i, i+time_resolution-1] delta_co2
//    co2_avg=V_avg
//    WaveStats/Q/R=[i, i+time_resolution-1] delta_polu

```

```

//      ratiowave[i+time_resolution-1]=V_avg/co2_avg
//      eventmarker[i+time_resolution-1]=0
//Elseif(self_count>=time_resolution*0.8)//self-measurements more than 80%
//      WaveStats/Q/R=[i, i+time_resolution-1] delta_co2
//      co2_avg=V_avg
//      WaveStats/Q/R=[i, i+time_resolution-1] delta_polu
//      ratiowave[i+time_resolution-1]=V_avg/co2_avg
//      eventmarker[i+time_resolution-1]=-1
Endif
Endfor
End

```

```

Function RatioConCat(wave_EF)
Wave wave_EF

String/G wavename_EF=NameofWave(wave_EF)
String/G species_EF=wavename_EF[3,strlen(wavename_EF)-1]
Sort wave_EF, wave_EF
WaveStats/Q wave_EF
Deletepoints V_npnts, V_numNaNs, wave_EF
StrSwitch (species_EF)
    Case "pah":
        ConcatenateWaves("EF_concatenated_pah",wavename_EF)
        Break
    Case "bc":
        ConcatenateWaves("EF_concatenated_bc",wavename_EF)
        Break
    Case "co":
        ConcatenateWaves("EF_concatenated_co",wavename_EF)
        Break
    Case "benzene":
        ConcatenateWaves("EF_concatenated_benzene",wavename_EF)
        Break
    Case "noy":
        ConcatenateWaves("EF_concatenated_noy",wavename_EF)
    Case "VOC":
        ConcatenateWaves("EF_concatenated_VOC",wavename_EF)
EndSwitch
End

```

```

//Function: Rescale_BC()
//Use: To rescale BC waves to the DustTrak (pm25) waves
//Original loaded wave, k4_bc_aeth, is 1-min spaced
//the DustTrak wave, d4_pm25_dt, provides the rescaling factor
//Input: string "mainpath"
//Auto-load: POI_pm25_dt.itx

```

Function **Rescale\_BC()**

```

SVAR mainpath=mainpath
Loadwave/a/d/o/t mainpath+"pm25_dt.itx"
Wave k4_bc_aeth=k4_bc_aeth, k4_bc_aeth_dataMask=k4_bc_aeth_dataMask
Wave d4_pm25_dt=d4_pm25_dt
DataMask(d4_pm25_dt)

Duplicate/o/d d4_pm25_dt, d4_bc_aeth
d4_bc_aeth=Nan
Variable i, n=numpts(k4_bc_aeth), jdex, startP,endP
For(i=0;i<n;i+=1)
    startP=x2pnt(d4_pm25_dt,pnt2x(k4_bc_aeth,i));endP=x2pnt(d4_pm25_dt,pnt2x(k4_bc_aeth,i+1))
    WaveStats/Q/R=[startP,endP] d4_pm25_dt
    For(jdex=0;jdex<60;jdex+=1)
        d4_bc_aeth[startP+jdex]=k4_bc_aeth[i]*(d4_pm25_dt[startP+jdex]/V_avg)
    Endfor
Endfor
String save_file=mainpath+"bc_aeth.itx"
Print "Save in", save_file
Save/O/B/T "d4_bc_aeth;k4_bc_aeth;k4_bc_aeth_NARSTO_tw;k4_bc_aeth_dataMask" as save_file

```

End

```

//Use: rescale PAH waves to the DustTrak (pm25) waves
//The PAH waves are the records of the analog output of PAS which is on one-second time series, but the analog output values are updated once every 5 secs ,
// and each signal represents an average of the previous 6 measurements.
//The rescaling is to pick out every updated values, one each 5 secs, and to interpolate for points in between.

```

```

//Input: string variable POI, mainfolder
//Output: d4_pah_pas_rs; save to //POIs//POI//d4_pah_pas_rs.itx
//Auto-load: d4_pah_pas, d4_pah_pas_dataMask

```

## Function **Rescale\_PAH()**

```
SVAR POI=POI //e.g. POI="M_20030413_PNT"  
SVAR mainfolder=mainfolder//note: mainfolder="C:\\Documents and Settings\\meij.CE\\My Documents\\Research\\"  
  
Loadwave/a/d/o/t mainfolder+"POIs\\"+POI+"\\"+POI+"_MITpart.itx"  
Wave d4_pah_pas=d4_pah_pas  
Wave d4_co2_licor1=d4_co2_licor1  
  
//Rescaled pah wave: d4_pah_pas_rs  
Duplicate/o/d d4_pah_pas, d4_pah_pas_rs_interp  
Make/o/d/n=(numpnts(d4_pah_pas)) d4_pah_pas_rs, d4_pah_pas_rs_time  
d4_pah_pas_rs=NaN  
d4_pah_pas_rs_time=NaN  
Variable i, n=numpnts(d4_pah_pas),j=0  
  
//Rescaling  
For(i=0;i<n;i+=1)  
    If(abs(d4_pah_pas[i]-d4_pah_pas[i-1])>1&&abs(d4_pah_pas[i+1]-d4_pah_pas[i])<1)  
        Do  
            d4_pah_pas_rs[j]=d4_pah_pas[i]  
            d4_pah_pas_rs_time[j]=pnt2x(d4_pah_pas, i)  
            j+=1  
            i+=5  
        While(i<=n)  
    Endif  
Endfor  
Deletepoints j, n-j, d4_pah_pas_rs, d4_pah_pas_rs_time  
  
For(i=0;i<n;i+=1)  
    d4_pah_pas_rs_interp[i]=interp(pnt2x(d4_pah_pas, i), d4_pah_pas_rs_time, d4_pah_pas_rs)  
Endfor  
  
String save_file=mainfolder+"POIs\\"+"PAH\\"+POI+"_pah_pas_rs.itx"  
Save/O/B/T "d4_pah_pas_rs_interp" as save_file  
End
```